Sustainable Utilization of Whey By-Product For the Production of Biobutanol

A Technical Report submitted to the Department of Chemical Engineering

Presented to the Faculty of the School of Engineering and Applied Science
University of Virginia

In Partial Fulfillment of the Requirements for the Degree
Bachelor of Science in Chemical Engineering

May 6th, 2025

Technical Project Team Members
Sarah Bogdan
Aidan Decker
Andrew Ludwikowski
Carson Min
Elizabeth Wu

Advisor
Professor Eric Anderson, Department of Chemical Engineering

On our honor as University Students, we have neither given nor received unauthorized aid on this assignment as defined by the Honor Guidelines for Thesis-Related Assignments.

TABLE OF CONTENTS

SUMMARY

The growing need for renewable energy has sparked renewed interest in biobutanol, a biofuel known for its high energy content and compatibility with current fuel infrastructure. Meanwhile, the increasing popularity of Greek yogurt in the U.S. has led to a rise in acid whey production, a by-product that, while rich in nutrients, presents significant environmental challenges. Improper disposal of whey can lead to water pollution, and existing methods of managing it are often costly and ineffective. One potential solution is converting whey into biofuel through fermentation, which not only addresses waste management issues but also contributes to the production of renewable energy. Thus, in the following report, we present the design of a processing plant that produces dry whey protein and biobutanol from the acid whey feedstock sourced from a major yogurt manufacturing plant.

The facility consists of upstream processing, fermentation, and separations and is designed to operate continuously for 24 hours a day, 330 days a year. In the upstream portion, ultrafiltration, spray drying, and reverse osmosis units are operated to process 27,215 kg/hr of acid whey, produce 969 kg/hr of dry whey protein, and concentrate a lactose-rich permeate stream. The lactose acts as a sugar for the *Clostridium acetobutylicum* during the acetone-butanol-ethanol fermentation process, which utilizes ten 50,000 L tanks on a 48 hour schedule supplemented by a seed train. Carbon dioxide is continuously purged during the fermentation. The fermented mixture is then sent to a depth filtration system to remove biomass, and finally, a five column distillation matrix to produce upwards of 140 kg/hr of biobutanol.

This project is not only a feasible method of waste management and renewable energy production but a profitable one as well. Cash flow analysis reveals that despite the capital-intensive early years, the plant will break even in five years and continue to generate

steady positive cash flow over its twenty year lifetime. Moreover, with a $0.70/kg tax credit for biobutanol or a focus on dry whey protein production only, the plant's financial return could further increase, though at the expense of the aforementioned environmental and social benefits. Overall, our findings stand to support the construction of such a plant, though further research and process optimization are always of value.

I. INTRODUCTION

The increasing demand for renewable energy sources has driven interest in biobutanol, a biofuel with high energy density and compatibility with existing fuel infrastructure. Biobutanol has a long history as a renewable fuel, first gaining attention during the early 20th century. It was initially produced through the ABE (acetone-butanol-ethanol) fermentation process, pioneered by Chaim Weizmann during World War I to produce acetone for explosives. In the post-war period, butanol production became economically unfavorable due to the rise of petrochemicals, which offered cheaper methods for producing acetone and butanol (Freemantle, 2017). With the advent of the petroleum industry, biobutanol production largely declined, though it experienced brief resurgences during oil shortages. The recent revival of interest in biobutanol production is driven by increasing awareness of climate change and the need to transition from fossil fuels to renewable energy sources. Additionally, advancements in biotechnological processes have made it feasible to produce butanol more efficiently than in the past.

Over the past decade, there has been a notable increase in American dairy consumption, particularly in Greek yogurt, driven by growing awareness of its health benefits. While Greek yogurt is rich in protein, essential nutrients, and beneficial probiotics, its production results in whey, a by-product that is both nutrient-dense and environmentally challenging. The disposal of whey is problematic due to its high biological oxygen demand and chemical oxygen demand, which can have detrimental effects on aquatic life and contribute to water pollution. Existing disposal methods of acid whey are often expensive, energy-intensive, and inadequate in handling the scale of production, leading some dairy companies to resort to improper disposal practices. One promising solution to these waste management issues involves converting whey into biofuel through fermentation in fermentation reactors.

This project focuses on converting acid whey, a by-product of Greek yogurt production, into biobutanol and whey powder. The process will be designed around the waste disposal of the largest yogurt manufacturing plant in the world: the Chobani facility in Twin Falls, Idaho. By repurposing the waste stream, the process not only mitigates environmental disposal challenges but also generates a valuable renewable fuel capable of powering over 1,300 vehicles annually. By utilizing the acetone-butanol-ethanol (ABE) fermentation process with *Clostridium acetobutylicum*, the high lactose content of acid whey is leveraged for efficient fermentation and biobutanol production. Moreover, the design is relatively safe, with the primary concerns related to this process involving the flammable material in the downstream operations. Furthermore, the positive environmental impact of this project aligns with the global shift away from fossil fuels and supports a circular economy by transforming waste into both energy and high-protein products.

II. PREVIOUS WORK

2.1 Whey to Biofuels

An estimated 1.5 million tons of acid whey were produced in 2015 due to the rising demand for Greek yogurt and cheeses (Erickson, 2017). Due to the problematic nature of acid whey disposal, several solutions have been explored to ferment the waste into a valuable alternative energy source. Most previous works involve whey-to-fuel ethanol production, which has been proven to be both technically and economically feasible. Starting in 1978, Carbery Milk Products Ltd. built the first whey-to-ethanol plant to produce commercial grade ethanol from whey permeate in Ireland (Ling, 2008). As of 1980, two industrial size whey-ethanol plants are currently operated in the United States (Ling, 2008). Though these two plants have been in operation for more than 20 years, there is a lack of publicly available production-cost data and no associated profitability estimates due to the challenges of the feedstock appraisal (Ling, 2008).

The steps for whey to biofuels are, for the most part, standardized. First, ultrafiltration separates the proteins from the acid whey. Next, reverse osmosis concentrates the lactose content before it is sent to fermentation. Post-fermentation, the liquid is sent to distillation columns to extract ethanol. The stillage and spent yeast are typically discharged into a treatment system but may be sold as feed or processed further into other products. This project follows a similar formula for biofuel production, though the aim is to produce butanol rather than ethanol. We also attempt to perform a complete economic appraisal, taking into consideration all capital and operating costs to evaluate if this truly is an economically viable endeavor.

2.2 ABE Fermentation

Alcohol-butanol-ethanol fermentation of carbohydrates such as starch and glucose is a well-established industrial process dating back to the early 1900s. The most well-studied bacteria strains that carry out the fermentation are *Clostridium acetobutylicum*, followed by *Clostridium beijerinckii* and *Clostridium saccharobutylicum.* A variety of feedstocks have been researched, such as plant-based feedstocks, sugary juices, and dairy by-products (Khamaiseh et al., 2014). Most recent research studies address methods of increasing product titer, productivity, and yield via adjusting operating conditions and selecting different strains (Lin et al., 2023). This project builds off of gathered fermentation model kinetics to design a working reactor model for the less commonly researched feedstock of acid whey.

2.3 Separation Designs

The process of ABE fermentation has long been studied for uses in producing acetone during World War 1 and butanol in the following years. Five column distillation matrices are the primary process utilized for purifying a fermentation broth into each of its components. These five column matrices have been well studied and documented, and, for the purposes of this project, they have served as an example model. Specifically the ABE fermentation process studied by Van Der Merwe was used for modeling initial column parameters in Aspen Plus Software (Blignault Van Der Merwe et al., 2010). Other studies were examined for alternative separation matrices, which ultimately resulted in the final design (Liu et al., 2022).

III. DISCUSSION

3.1 Overall Design Basis

The basis for this process is the Greek yogurt production at Chobani's Twin Falls, ID facility. The approximated acid whey feed stream was found to be 27,215 kg/hr at this Chobani plant, with calculations detailed in Appendix A (Charles, 2012). The feed stream consists of water, whey protein, lactose, and solvated salts. An ultrafiltration system is the first unit operation that the feed stream is passed through. Ultrafiltration is a membrane-based separation process that uses size to divide the feed stream into two exiting flows. Larger molecules, principally proteins, are held in the retentate of the ultrafiltration membrane, while lactose, water, and other small molecules permeate through the membrane. The protein-rich stream is sent to a spray dryer where it is atomized into a hot air stream. Lowering the moisture content of the whey protein allows for it to be sold as a valuable product in bulk. The remaining permeate is sent to a reverse osmosis system, a pressure-driven process that removes water and concentrates the lactose before fermentation. Concentrating the lactose to about 10 wt% (Paredes et al., 2021) offers conditions that maximize the productivity of fermentation. During ABE fermentation, *Clostridium acetobutylicum* ferments lactose into acetone, butanol, and ethanol through a two-stage anaerobic process. Acidogenesis produces butyric and acetic acid as intermediate products, and solventogenesis converts these acids into the solvent products. Butanol is the desired product, and the system is optimized to produce high concentrations of the biofuel. The fermented substrate is taken through a depth filtration system where cell debris and other solids are removed before distillation can separate the mixture. A system of five distillation columns will be used to carefully isolate acetone, butanol, and ethanol, while water and carbon dioxide exit as waste streams. The acetone and butanol produced are pure enough to be sold in bulk and will be our principal products from this process. A basic flow diagram with the intended flow rates can be seen in *Figure 3.1-1*.

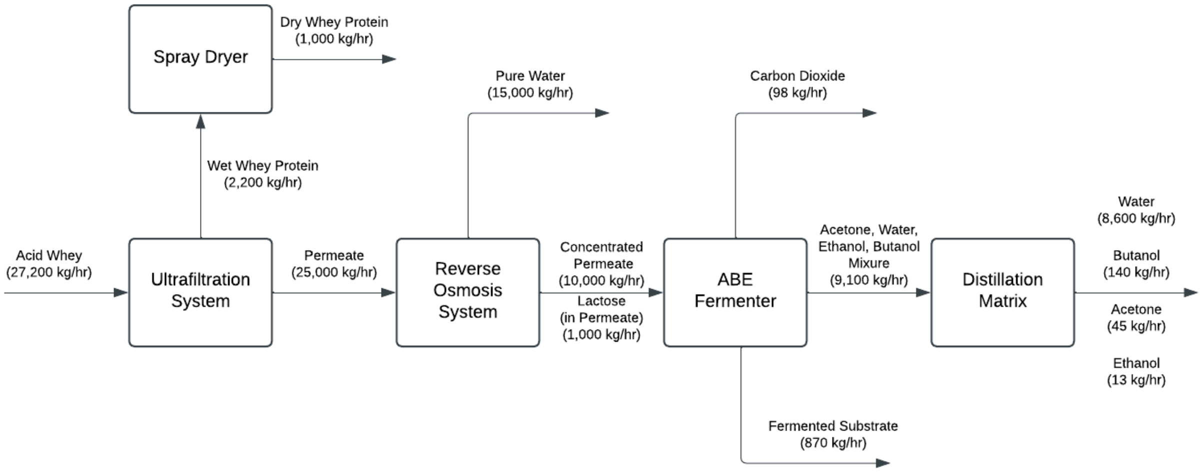

Figure 3.1-1 Basic BFD for Solvent Production from Acid Whey

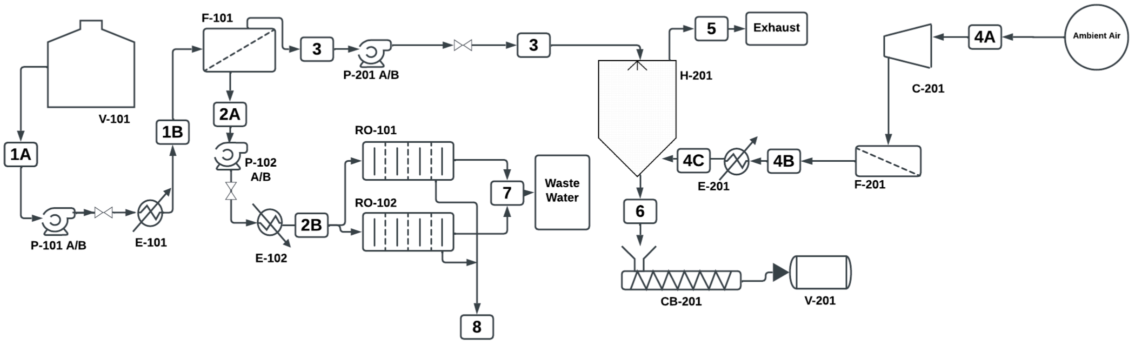

Figure 3.1-2 Upstream Process Flow Diagram

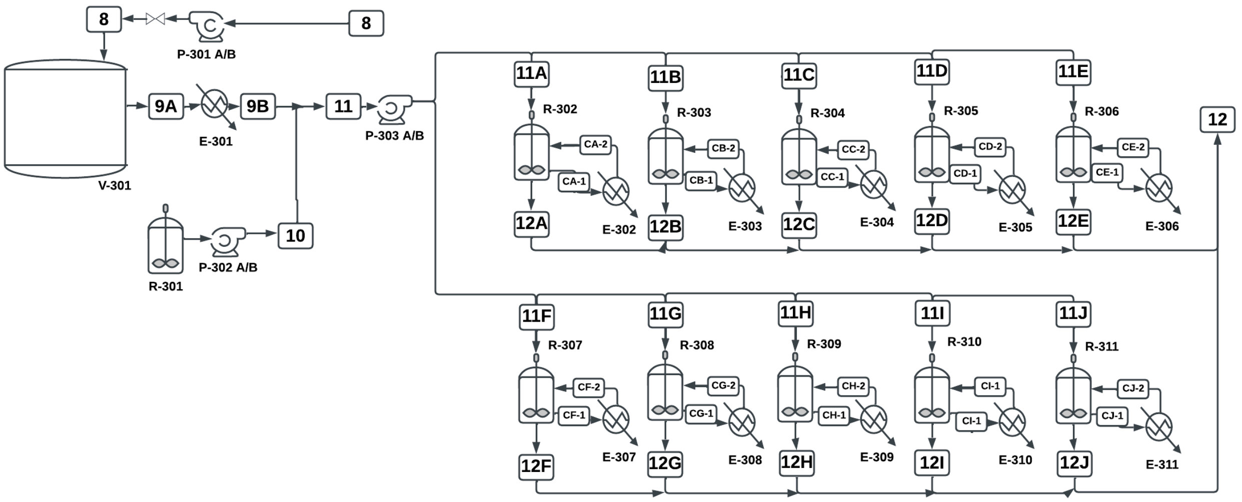

Figure 3.1-3 Fermentation Process Flow Diagram

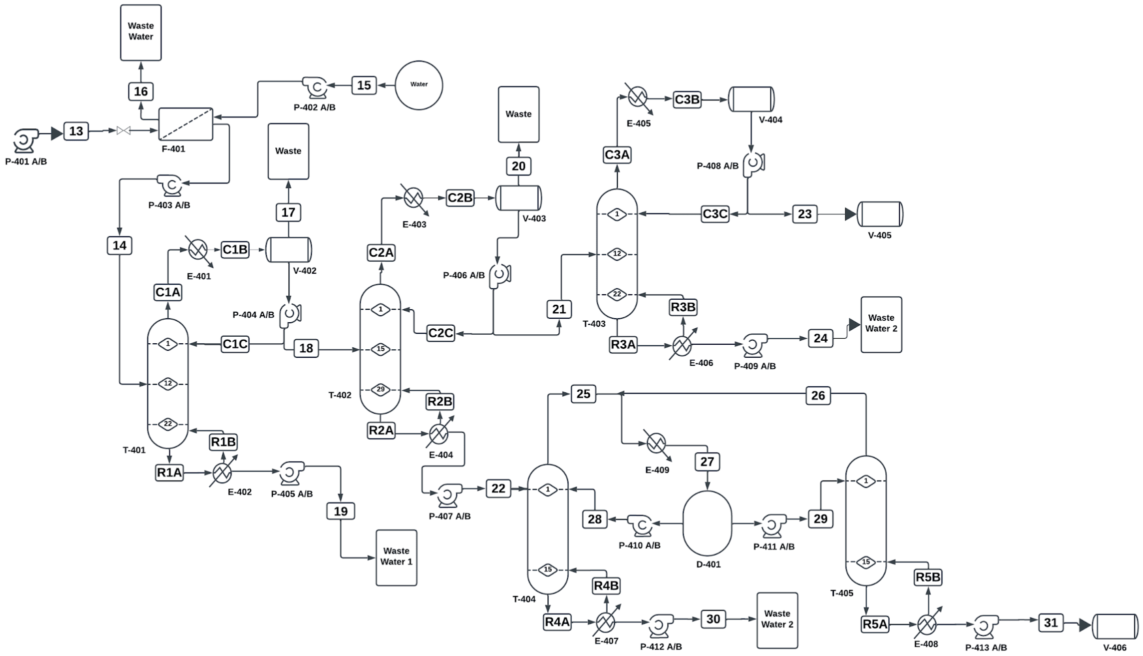

Figure 3.1-4 Separation System Process Flow Diagram

3.2 Ultrafiltration System

3.2.1 Unit Design

Ultrafiltration (UF) utilizes a small pressure differential to separate whey proteins from the liquid feed through a semipermeable membrane with a molecular weight cutoff (MWCO) of 10 kDa (Safe Drinking Water Foundation, 2025). The system of choice (F-101) is a single-pass tangential flow filtration (SPTFF) system designed to process acid whey feedstock at a flow rate of 27,215 kg/hr and an inlet temperature of 48°C. This system employs a tangential filtration approach to prevent particle buildup on the membrane by maintaining a continuous flow of fluid along its surface. The membrane of choice is the Synder Filtration ST 10 kDa Sanitary UF Membrane, which is made of polyethersulfone (PES) (Synder Filtration, n.d.). PES is a material characterized by a high resistance to fouling, a good resistance to pH and temperature, and compliance to USDA sanitary standards, which is crucial for ensuring the safety of products meant for human consumption (Synder Filtration, n.d.). Further specifications and dimensions for the membrane are represented in *Table 3.2-1*.

3.2.2 Pressure Drop

The osmotic pressure, π , was calculated in units of atm via *Equation 3.2-1.* c_s represents the retentate protein concentration in grams per liter and is found to be 16 g/L from literature running a similar experiment at maximum volume concentration (El-Gazzar & Marth, 1991). Assuming complete protein rejection, the osmotic pressure will be equivalent to the osmotic pressure differential.

$$\textbf{(Eq. 3.2-1)}\ \pi = \Delta\pi = 4.4 * 10^{-3}(c_s) - 1.7 * 10^{-6}(c_s)^2 + 7.9 * 10^{-8}(c_s)^3$$

This value is relatively low, which is typical for a UF system, as UF generally operates with modest osmotic pressures compared to other filtration processes like reverse osmosis. The permeate flux in m/s, u, and the water flux per unit pressure drop in m/(s*bar), Q_m, were chosen based on industry standards (McCabe et al., 1993). The driving force for filtration is found via *Equation 3.2-2* and is useful to note as it directly drives the separation process. Based on the calculations performed in *Equation 3.2-3*, a pressure differential of 0.52 bar is required to meet such demands and ensure efficient filtration. The system operates with an inlet pressure of 1.6 bar and an outlet pressure of 1.0 bar.

(Eq. 3.2-2) $$driving\ force = \Delta P - \Delta\pi$$

(Eq. 3.2-3) $$\Delta P = \frac{u}{Q_m} + \Delta\pi$$

Table 3.2-1 Ultrafiltration Unit (F-101) Specifications

Parameter	Value
Membrane material	Polyethersulfone
MWCO	10,000 Da
Feed mass flow rate	27,215 kg/hr
Diameter	20 cm
Length	102 cm
Membrane area	34.2 m^2
Recommended element cross flow rate	24 m^3/hr
Inlet pressure	1.6 bar
Outlet pressure	1 bar
Operating temperature	48°C

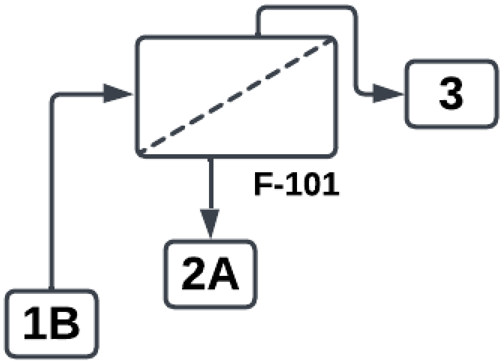

Figure 3.2-1 Ultrafiltration System Process Flow Diagram

3.3 Spray Dryer

3.3.1 Unit Design

The spray dryer (H-201) is designed to dry the concentrated whey protein stream from the ultrafiltration system, producing a final powder with a maximum moisture content of 3.5%. This process is essential for improving the storage stability and marketability of the whey protein powder. A counter-current spray drying system is employed, where the whey feed stream is atomized into fine droplets at the top of the drying chamber using a rotary atomizer. Simultaneously, hot air enters from the bottom and moves upward, facilitating the drying process by maximizing heat transfer and moisture removal (PowderProcess.net, n.d.).

The feed stream enters the system at 48°C , with a total solid content of 43%, and is dried to an outlet temperature of 48°C. The inlet air is heated to 180°C, while the outlet air temperature is reduced to 80°C before being exhausted with a relative humidity of 15%. Although many proteins denature at high temperatures, whey protein can handle higher temperatures, such as 180°C utilized here. (PowderProcess.net, n.d.). The mass flow rates and moisture balances ensure that the system operates efficiently while meeting product specifications. The feed and drying process parameters are summarized in *Table 3.3-1*.

Table 3.3-1 Spray Dryer (H-201) Process Conditions

Parameter	Value
Total feed mass flow rate	2,253 kg/hr
Feed total solid	43%
Feed temperature	48ºC
Outlet solids moisture	3.50%
Outlet solids temperature	48ºC
Atmospheric air temp	25ºC
Atmospheric air relative humidity	50%
Inlet air temperature	180ºC
Outlet air temperature	80ºC
Exhaust air relative humidity	15%

3.3.2 Process Conditions and Material Balances

The material balance for water removal is established using the mass flow rates of air, feed, and final dried powder, as shown in *Equation 3.3-1*. Using the values provided in *Table 3.3-2*, the required air flow rate, G_A, was determined to be 33,730 kg air/hr, which was then validated against industry standards and literature calculations (Mujumdar & Jog, 1977).

$$\textbf{(Eq. 3.3-1):}\ G_A \bullet H_1 + M_S \bullet Ws_1 = G_A \bullet H_2 + M_S \bullet Ws_2$$

Table 3.3-2 Spray Dryer Material Balance Specifications

Parameter	Value
Dry Solid mass flow rate, M_s	969 kg solids/hr
Moisture in the feed, Ws_1	1.33 kg water/kg solids
Moisture in the outlet solids, Ws_2	0.04 kg water/kg solids
Inlet air absolute humidity, H_1	0.0098 kg water/kg air
Outlet air absolute humidity, H_2	0.0468 kg water/kg air

3.3.3 Rotary Atomizer and Droplet Formation

The rotary atomizer ensures uniform droplet formation, optimizing drying efficiency. The design specifications for the atomizer are summarized in *Table 3.3-3*. The design procedure simply consists of choosing reasonable values for wheel diameter (d), wheel speed (n), and vane height (h) that will result in $0.9 < M_p < 5.4$ in *Equation 3.3-2*. A value of 29.4×10^4 microns was used for K, an empirical constant that accounts for the combined effects of various operational and equipment-related factors on the droplet size in a spray dryer, as per industry standards for operations of this scale (Mujumdar & Jog, 1977). Droplet size was calculated using *Equation 3.3-3*.

Table 3.3-3 Rotary Atomizer Design Parameters

Parameter	Value
Wheel diameter, d	0.22 m
Wheel speed, n	15,000 rpm
Number of vanes, N	20
Vane height, h	0.02 m
Mass Flow Rate, M_L	2,253 kg/hr
Droplet size, D_{vm}	11.72 microns

(Eq. 3.3-2): $M_p = (\frac{M_L}{nh})$

where:

Variable	Range of Operation
Wheel diameter (cm)	19.0 - 23.0
Wheel speed (rpm)	10,000 - 18,000
M_p = liquid loading on vane	0.9 - 5.4

(Eq. 3.3-3): $D_{vm} = \frac{K(M_L)^{0.24}}{(Nd)^{0.83}(nh)^{0.12}}$

3.3.4 Chamber Design Specifications

The spray drying chamber is designed to ensure space and time for the droplets to completely dry before reaching the collection point. The chamber size is determined based on the maximum radial dispersion of droplets, which governs the droplet path length and, ultimately, the height required for complete moisture removal. The maximum dispersion radius (R_{max}) and 99% dispersion radius (R_{99}) were calculated in meters using the empirical equations from Frazier, Eisenklam, Dombrowski, and Herring & Marshall, seen as *Equation 3.3-4* and *Equation 3.3-5*. R_{max} is the radial distance at which 99% of the spray falls 0.91 meters below the atomizer, and R_{99} is the radial distance which includes 99% of the mass of the spray (Mujumdar & Jog, 1977). These values are calculated in meters using the values in Table 3.3-3. These equations determined different radial predictions, so to account for this variability, the average was taken to determine the radius of the chamber. In practice, pilot plant data should be taken into account to determine a more accurate radius specification. The values from these equations and the determined radius can be found in *Table 3.3-4*. This average dispersion radius was used as the basis for the chamber diameter. The final diameter, D_c, was determined to be 7.25 m.

(Eq. 3.3-4): $R_{max} = 7.48\frac{d^{0.21}M^{0.2}}{N^{0.16}}$

(Eq. 3.3-5): $R_{99} = 11.87\frac{d^{0.2}M^{0.25}}{N^{0.16}}$

Table 3.3-4 Chamber Radius Calculations

Parameters	Values
Maximum dispersion radius (R_{max})	2.467 m
99% dispersion radius	4.779 m
Average radius	3.62 m

With the chamber diameter determined, the chamber height can be determined using *Equation 3.3-6* and *Equation 3.3-7*. *Equation 3.3-6* calculates dry air velocity (v) inside the chamber, using the chamber diameter (D_c), the air flow rate (G_A), and the specific volume of air (V_B). The specific volume of air used at 180°C was 1.285 m^3/kg (Engineering ToolBox, n.d.). The calculated air velocity is 0.230 m/sec. This value was then used in *Equation 3.3-7* along with the industry-standard residence time of 30 seconds to determine the chamber height to be 8.83 m, ensuring the droplets have adequate time to dry before reaching the bottom of the chamber (Mujumdar & Jog, 1977).

$$\textbf{(Eq. 3.3-6) } v = \frac{4}{\pi D_c^2}(G_A V_B)$$

$$\textbf{(Eq. 3.3-7) } chamber\ Height = v * residence\ time$$

A full summary of the spray dryer chamber dimensions can be found in *Table 3.3-5*.

Table 3.3-5 Spray Dryer Chamber Dimensions

Parameter	Value
Inlet air velocity	0.230 m/sec
Residence time	30 sec
Chamber diameter	7.25 m
Chamber height	8.83 m

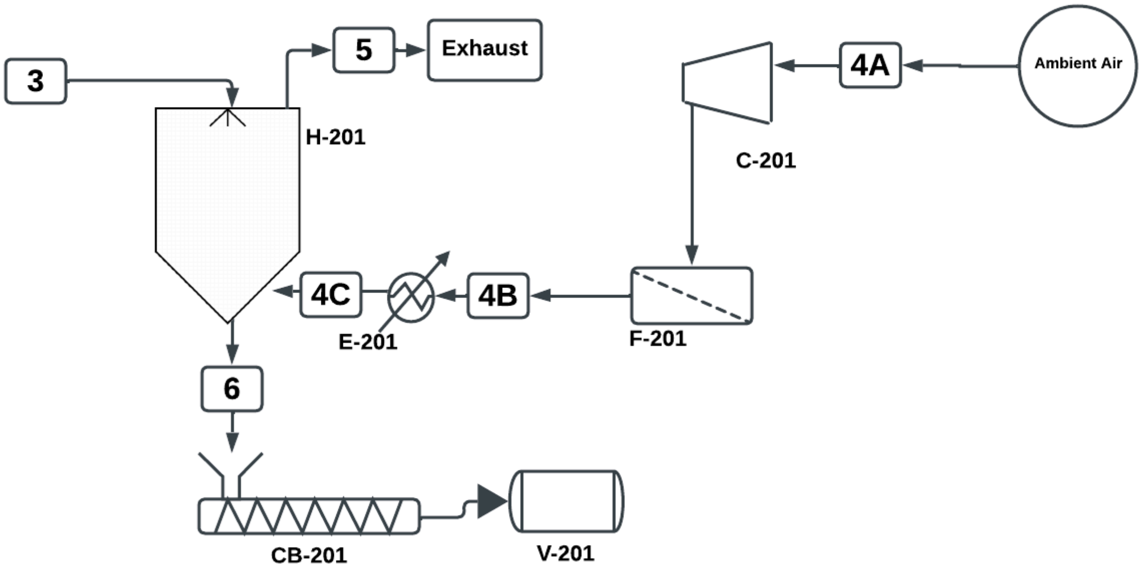

Figure 3.3-1 Spray Dryer Process Flow Diagram

3.3.5 Energy Balance

The energy balance for the spray dryer accounts for the thermal energy required to evaporate moisture from the whey protein feed and the power required for atomization. The primary energy components include:

1. Latent Heat of Evaporation – The energy required to remove moisture from the feed.
2. Rotary Atomizer Power – The energy required for the atomization of the feed into fine droplets.

The latent heat of evaporation is determined based on the mass of water removed and the latent heat of vaporization of water. Given the feed rate and initial and final moisture contents in *Table 3.3-6*, the mass flow rate of water removed was calculated to be 1249 kg/hr or 0.35 kg/s using *Equation 3.3-8*. Using the heat of vaporization of water, 2,260 kJ/kg (Datt, 2011), the latent heat of evaporation of the water was calculated using *Equation 3.3-9* to be 791 kW. The rotary atomizer disperses the whey protein feed into fine droplets, ensuring efficient drying. For industrial-scale operations, rotary atomizers typically consume about 30 kW of power.

Table 3.3-6 Latent Heat of Evaporation Calculation Parameters

Parameters	**Values**
Wet whey feed rate, m	2253 kg/hr
Initial wet whey moisture content, X_{in}	53%
Final whey moisture content, X_{out}	3.5%

(Eq. 3.3-8) $m_w = m \cdot \frac{X_{in} - X_{out}}{1 - X_{out}}$

(Eq. 3.3-9) $Q_{evap} = m_w \cdot H_{vap}$

3.4 Reverse Osmosis System

3.4.1 Unit Design

Reverse osmosis (RO) is primarily used to filter salts and other minerals from drinking water, but in this case, it will be used to concentrate the lactose content in the incoming filtered whey stream. The stream enters at 25°C at a flow rate of 24,962 kg/hr into the RO units (RO-101 and RO-102). The lactose concentration in the inlet is 39.8 g/L (3.98%), and 99.5 g/L (9.95%) at the outlet, a level determined to be suitable for ABE fermentation (El-Gazzar & Marth, 1991). The configuration chosen is the Hydranautics DairyRO 8040 30 Sanitary Membrane, which is a spiral wound system commonly used for whey concentration with a MWCO of 200 Da (*DiaryRO*, n.d.; Safe Drinking Water Foundation, n.d..). A complete specification of the membrane can be referenced in *Table 3.4-1*.

3.4.2 Pressure Drop

The osmotic pressure was found using *Equation 3.4-1* below, where C_f and C_R are the lactose concentrations of the feed and retentate streams, respectively, T is the temperature of the feedstock in Kelvins, and R is the gas constant:

$$\textbf{(Eq. 3.4-1)}\quad \Delta\pi = (C_R - C_f)RT$$

The permeate flux was calculated via *Equation 3.4-2*, where Q_w is the total feed volumetric flow rate and N is the number of RO units required. A is the total wetted membrane area (m^2) and is based on the design of a specific Hydranautics membrane designated for dairy product processing (*DiaryRO*, n.d.). Based on the permeate flux calculations and the maximum feed flow rate set by the model membrane, it was determined that two RO systems in parallel, consisting of one membrane each, will be necessary to process the desired flow rate. The final pressure drop was found to be 58 bar, and thus, the inlet pressure of 60 bar and outlet pressure of 1 bar were chosen as such.

$$\textbf{(Eq. 3.4-2)}\ J_w = \frac{Q_w}{N*A}$$

$$\textbf{(Eq. 3.4-3)}\ \Delta P = \frac{Q_w}{K_w} + \Delta\pi$$

Table 3.4-1 Reverse Osmosis Unit (RO-101 and RO-102) Specifications

Parameter	Value
Membrane material	Polyamide
MWCO	200 Da
Feed mass flow rate	24,962 kg/hr
Diameter	20.1 cm
Membrane permeability	6 L/(bar*m^2*hr)
Membrane Area	36 m^2
Inlet pressure	60 bar
Outlet pressure	1 bar
Operating temperature	25°C

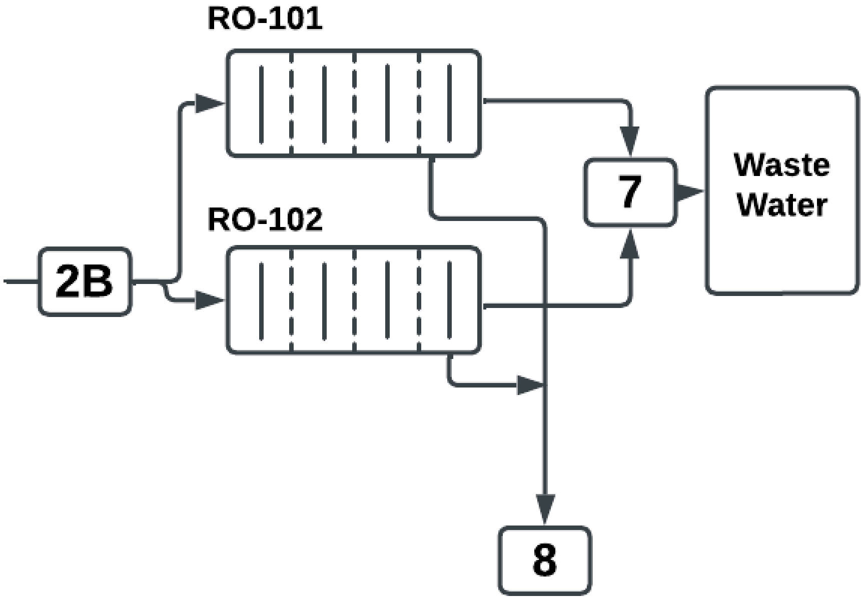

Figure 3.4-1 Reverse Osmosis System Process Flow Diagram

3.5 ABE Fermentation Reactors

3.5.1 Unit Design

Fermentation is a ubiquitous industrial process in which microorganisms break down substrates, usually sugars, into valuable commodities, including alcohol, gases, and other chemical products. From the perspective of the dairy industry, lactose is a fermentable sugar that has the potential to create a variety of edible dairy products. ABE fermentation is a type of fermentation in which bacteria can specifically break down substrates to yield acetone, butanol, and ethanol. These solvents are valuable products and are important to provide alternatives to fossil fuels. ABE fermentation consists of an initial acidogenesis phase where lactose can be broken down first into acetic acid and butyric acid. The increased acidity of these intermediate products as compared to the initial substrate favors the formation of the aforementioned solvents, resulting in a 3:6:1 molar ratio of acetone, butanol, and ethanol (Cheng et al., 2022). To maintain atmospheric pressure in fermentation vessels, carbon dioxide is continuously released through a vent. This release has been measured and is modeled in the associated fermentation stream tables as combined vapor release in Appendix B.

The process used in this study will incorporate a pre-filtered lactose feed solution and will be fermented by *Clostridium acetobutylicum*, a strain of bacteria that is well-studied to yield high concentrations of butanol as a product. Fermentation tanks will be held at a steady temperature of 35ºC and atmospheric pressure to maximize the productivity of *C. acetobutylicum* (Md Razali et al., 2018). To account for the scale of production, it was calculated that ten 50,000 L tanks are required to adequately conduct fermentation, shown in *Figure 3.5-5*. A large tank will hold the lactose solution prior to fermentation, which will contain up to a volume of 800,000 L. This allows the tank to hold more than three days worth of retentate and will help to prevent the overflowing of fermentation tanks. Individual fermenters will have a 3.61 meter diameter and a 5.49 meter height. In industrial settings, it is standard to size impellers as one-third of the diameter of individual vessels; therefore, the impeller diameters will be set to 1.2 meters (Afshar Ghotli et al., 2020). Rushton impellers have been experimentally shown to best mix cells and substrates during ABE fermentation without rupturing cells, so a Rushton impeller was chosen for operation (Junker et al., 1998).

3.5.2 Andrews Kinetics Model Parameters

ABE fermentation can be modeled using Monod kinetics to approximate the amount of product made as a function of substrate concentration, bacteria concentration, and yield factors. Substrate inhibition is another important factor to consider when making design equations, as high substrate concentrations lower the activity of microbes, increase the viscosity of the liquid, and make oxygen transport in the reactor more inefficient (Zhang et al., 2015). Therefore, the Andrews kinetics model provides a model that accounts for substrate inhibition and was chosen. The half-saturation constant (K_S) gives the determined concentration at which cell growth rate (μ) is at half of its max, setting a growth scale (Procentese et al., 2015). The inhibition constant (K_i) is the concentration where the substrate begins to inhibit production (Ezeji et al., 2004). The yield coefficients detail the mass of cells grown per substrate consumed ($Y_{X/S}$) and the mass of product produced per substrate consumed ($Y_{P/S}$) (Paredes et al., 2021).

Table 3.5-1 Andrews Kinetic Parameter Values

Component	Value
K_S	2.0 g/L
K_i	20 g/L
μ_{max}	0.26 h^{-1}
$Y_{X/S}$	0.0797 g/g
$Y_{P/S}$	0.225 g/g
X_0	1.0 g/L
S_0	99.5 g/L

Note: K_S from Darkwah et al. (2018); K_i from Procentese et al. (2015); μ_{max}, $Y_{X/S}$, and $Y_{P/S}$ from Paredes et al. (2021).

3.5.3 Simulation Output

A simulation of the Andrews Kinetics for ABE fermentation was completed via MATLAB. The differential growth rate of cells, substrate consumption, and product formation rate are described in Equation 3.5-1 through Equation 3.5-4. The parameters described above were then entered alongside the equations to model fully and graphically represent our fermentation process, as shown in Figure 3.5-2. The product output concentrations are reported in Table 3.5-3.

(Eq. 3.5-1) $$\mu = \frac{\mu_{max} S}{K_s + S + \frac{S^2}{K_i}}$$

(Eq. 3.5-2) $$\frac{dX}{dt} = \mu X$$

(Eq. 3.5-3) $$\frac{dS}{dt} = -\frac{1}{Y_{x/s}}\frac{dX}{dt}$$

(Eq. 3.5-4) $$\frac{dP}{dt} = -Y_{P/S}\frac{dS}{dt}$$

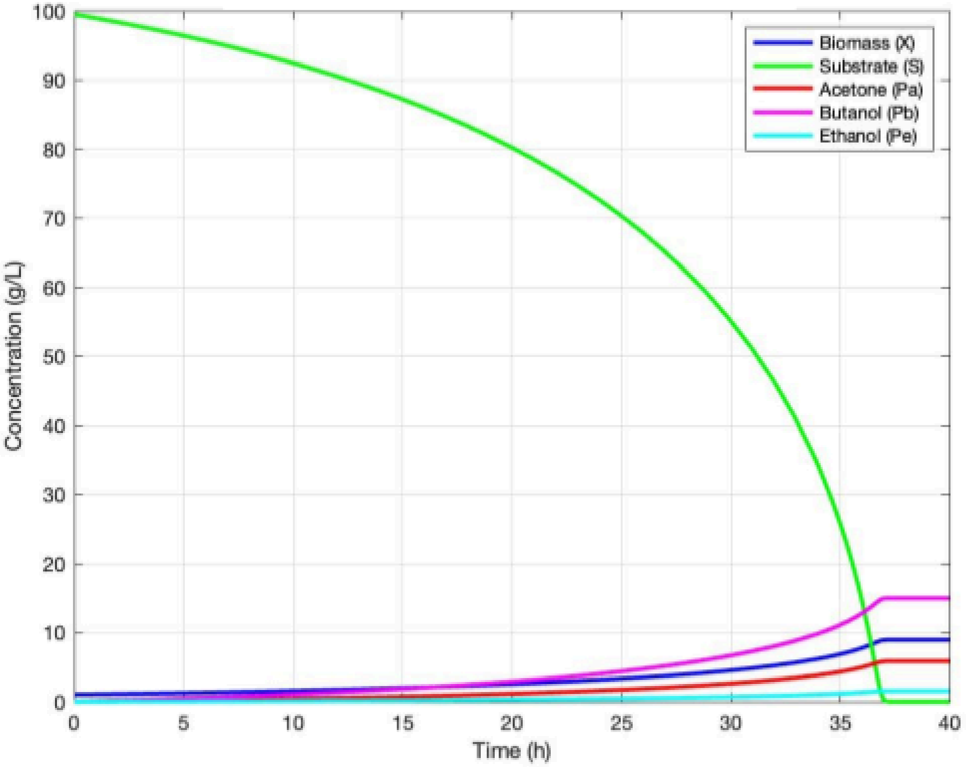

Figure 3.5-2 MATLAB Kinetic Model Results

Table 3.5-3 Kinetic Model Outlet Concentration Results

Component	Final Concentration
Lactose	0 g/L
Biomass	8.93 g/L
Acetone	5.87 g/L
Butanol	15.0 g/L
Ethanol	1.54 g/L

3.5.4 Reactor Schedule

To maximize the efficiency of fermentation reactors, a staggered schedule is recommended to give ample time to clean tanks, equalize product flow rates over time, and reduce the intensity of resource demands for downstream and fermentation processes. A 48 hour total cycling time allows for predictable, even scheduling for operators and plant leaders. As there are ten fermentation tanks, offsetting the cycle time of each tank by 4.8 hours accomplishes these set goals. The 48 hour cycle includes 4 hours of filling the tanks, 38 hours of fermentation, 4 hours of emptying the tanks, and 2 hours of cleaning in place (CIP). A complete schedule can be found in Figure 3.5-4.

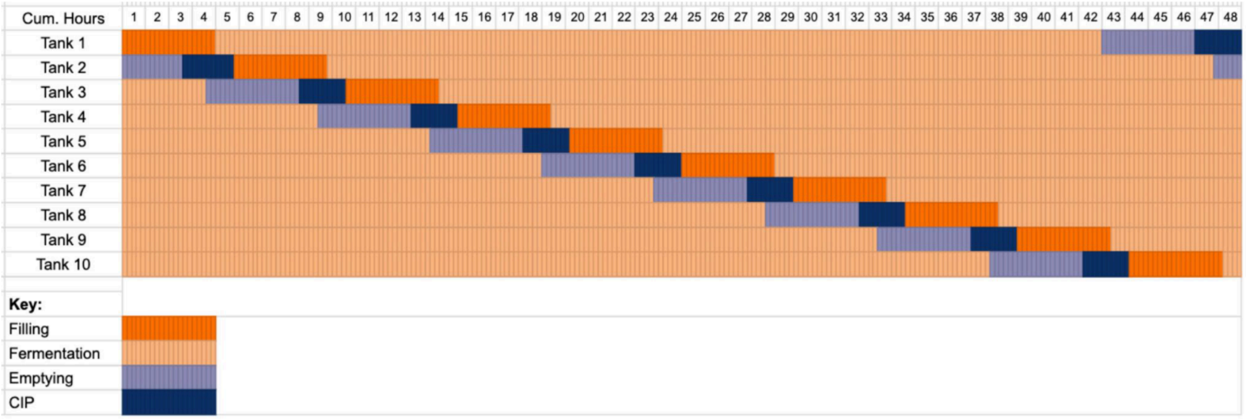

Figure 3.5-4 ABE Fermentation Schedule

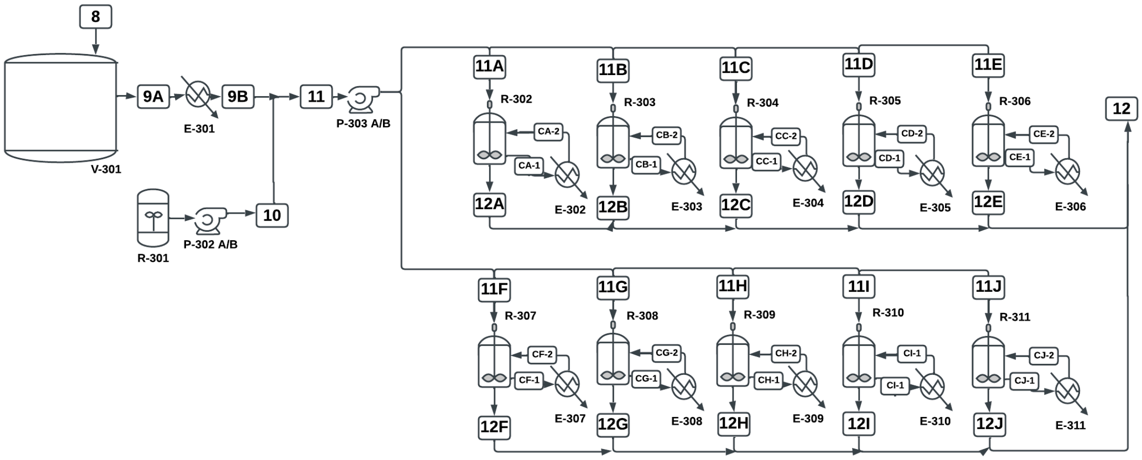

Figure 3.5-5 Fermenter Design Process Flow Diagram

3.6 Seed Train System

3.6.1 Unit Design

In order to scale fermentation to the industrial requirements detailed above, a seed train is required. Seed trains are systems of tanks that scale bacterial growth at increasing volumes until a saturated culture large enough to ferment commercial-sized tanks is achieved. Reactors in the seed train will be held at 35°C and atmospheric pressure, consistent with the fermentation tanks. Previous scale-up work involving *C. acetobutylicum* determined that sufficient inoculum volume for a seed train involving the bacteria is around 3-5% (Syed, 1994). This means that the concentrated bacteria moving between reactors should constitute 3-5% of the diluted volume used in the next reactor, showing that reactor volume scale-up should lay in the range of 20-33 times larger per fermentation. Another general assumption for cell growth is that there are approximately one billion cells per gram of broth (Hartline, 2022). As can be seen in *Figure 3.6-1*, *C. acetobutylicum* cells showed an increase from 10^7 cells/mL to 10^{10} cells/mL in a 24-hour period with a 25% glucose substrate (López-Contreras et al., 2022). This finding can be utilized in the seed train calculations to prove that *C. acetobutylicum* cells multiply by 1,000-fold in a 24-hour growth phase. A 1,000-fold increase in cell count corresponds to a 1,000-fold increase in cell mass, showing that a 1 g/L final concentration can be achieved with a three-stage seed train. Aggregating these assumptions gave enough information to determine that a three-stage seed train can yield enough bacteria to supply the 50,000 L tanks with 1 g/L of cells.

Working backwards from a 50,000 L fermentation reactor cell concentration of 1 g/L, the contents of a 50 L reactor with 1 kg/L of cells can supply this reactor with adequate *C. acetobutylicum*. Further working back using 1,000-fold growth over a 24-hour period and a 3% inoculum volume, 50 mL and 1.5 L reactors can provide the first two steps of the seed train.

Frozen stocks of *C. acetobutylicum* will be kept in enough excess to ensure that seed trains can be run continuously for all tanks. A swab from a frozen stock will be added to a 50 mL shake flask. After 24 hours of exponential growth, the cells will be moved to a 1.5 L bioreactor with a 6 cm agitating Rushton impeller. For the last step in the seed train, these cells 24 hours later will be transferred to a 50 L bioreactor and grown for a final 24 hours. A total time of 72 hours is required to scale up from a cell pellet to the solution ready for large-scale fermentation, which with overlapping schedules can produce cells for the fermentation tanks every 48 hours. To supply each of the ten 50,000 L fermentation tanks, an individual seed train is needed for each tank.

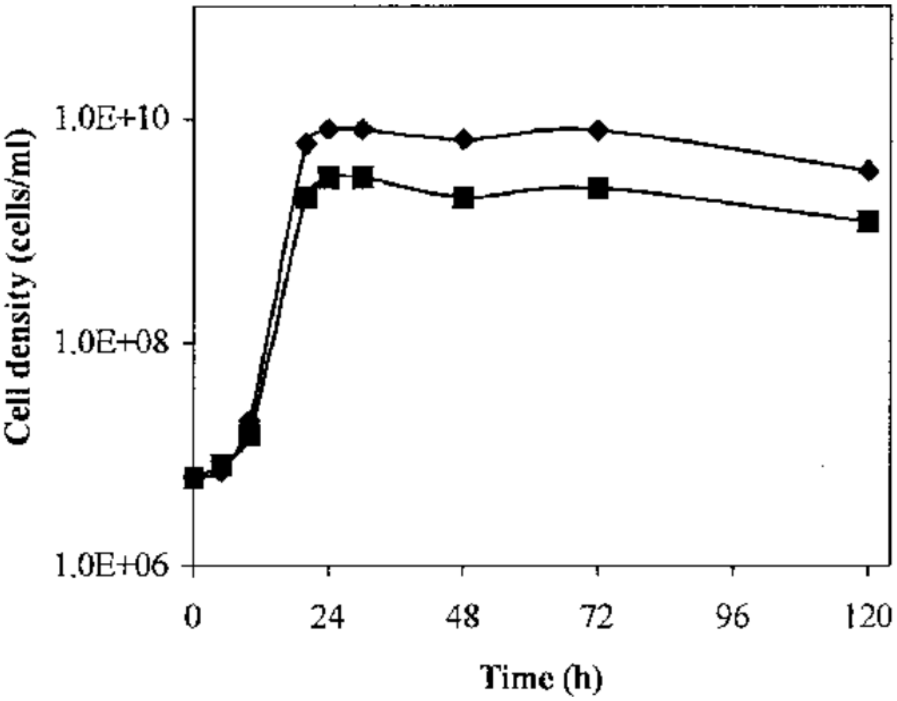

Figure 3.6-1 Average *Clostridium acetobutylicum* Growth Curve in 10% Hydrolysed DOW (López-Contreras et al., 2022)

3.6.2 Seed Train Schedules

A finished 50 L fermentation is required every 48 hours to allow for enough bacteria to keep ABE fermentation on a 48-hour schedule. To achieve this, 50 mL growth and 50 L growth are overlapped where tanks are immediately washed after use and available to be filled with more *C. acetobutylicum* (*Figure 3.6-2*). Tanks will each have a 24 hour period in which they can be washed, allowing ample time for operators to ready equipment for fermentation. To match the schedule shown in *Figure 3.5-4*, each of the ten seed trains must be staggered to match the staggered filling times of individual 50,000 L tanks. The schedule shown below in *Figure 3.6-3* helps visualize how 50 L cell growth will be matched to 50,000 L tank filling to meet production requirements, where every 48 hours a completed cell batch can be used to fill each fermenter.

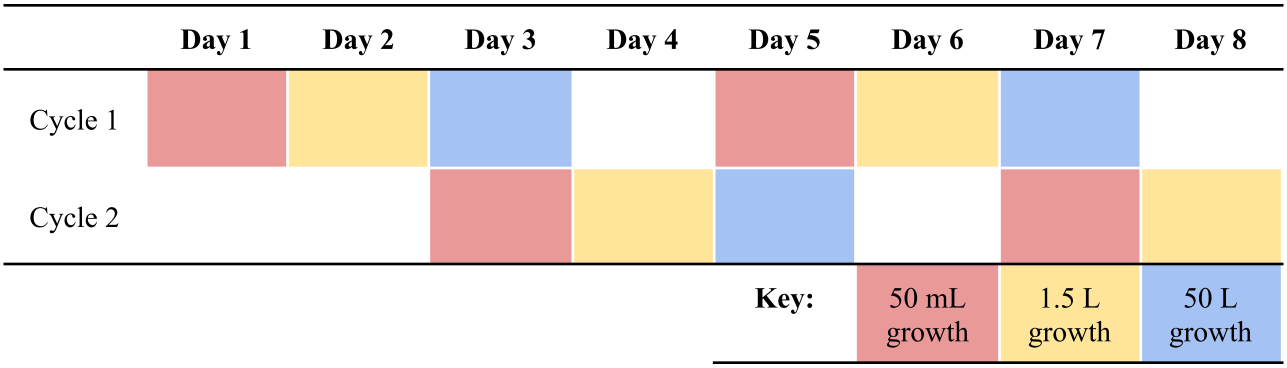

Figure 3.6-2 Individual Seed Train Reactor Schedules

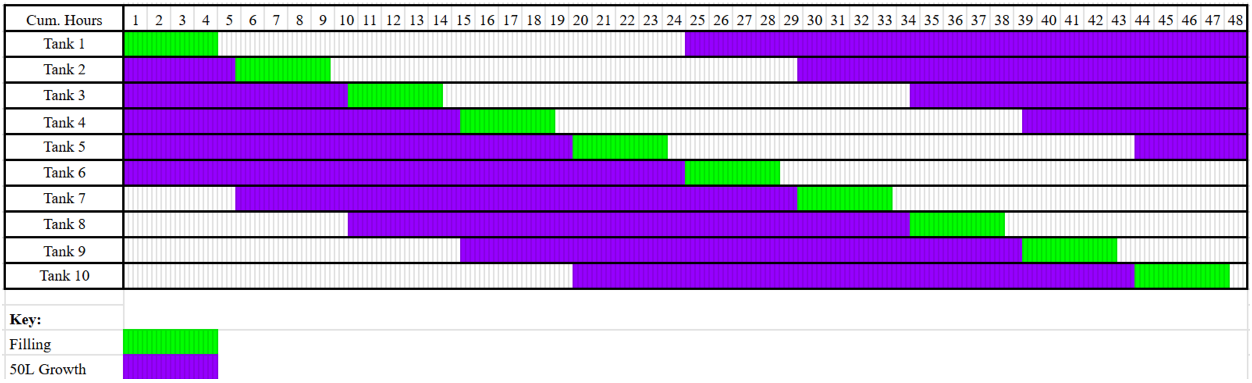

Figure 3.6-3 Overlay of Final Seed Train Scale-Up With Fermentation Tank Filling

3.7 Depth Filtration System

3.7.1 Unit Design

Depth filters are commonly used in bioprocessing, specifically for removing cells and debris from cell culture broths prior to separations. For the purposes of this process, a heavy-duty depth filtration system (F-401) consisting of two filters is used to clarify the broth to ensure more efficient separation processes later on. The broth enters at an inlet temperature of 35°C and a total flow rate of 8,932 kg/hr, a feed rate based on the mass from the fermenter divided by pump out time. The Reynolds Culligan Side Mount Depth Water Filter System will be used, which is specifically designed to capture a broad range of particulate sizes, handle high volumes of liquid, clog less, and offers a more cost-effective solution compared to ultrafiltration systems (Culligan International, 2004; Zydney & van Reis, 2011). The filter media of such capsules are made of cellulose rated at a pore size of 0.45 microns, which is adequate for the complete removal of *C. acetobucylicum* bacterium, which has a minimum size of 0.5 microns (Culligan International, 2004). For more efficient filtration, backwashing is performed to remove all biomass and build-up contained within the depth filters. A safe estimate for a backwashing schedule is once every 48 hours, with the backwashing process taking 30 minutes (Culligan International, 2004). During this time, the system will switch to the backup filter to ensure uninterrupted operation. A sample nine day backwashing schedule is represented in *Figure 3.7-1*. Additionally, further specifications and dimensions for the membrane are represented in *Table 3.7-1*.

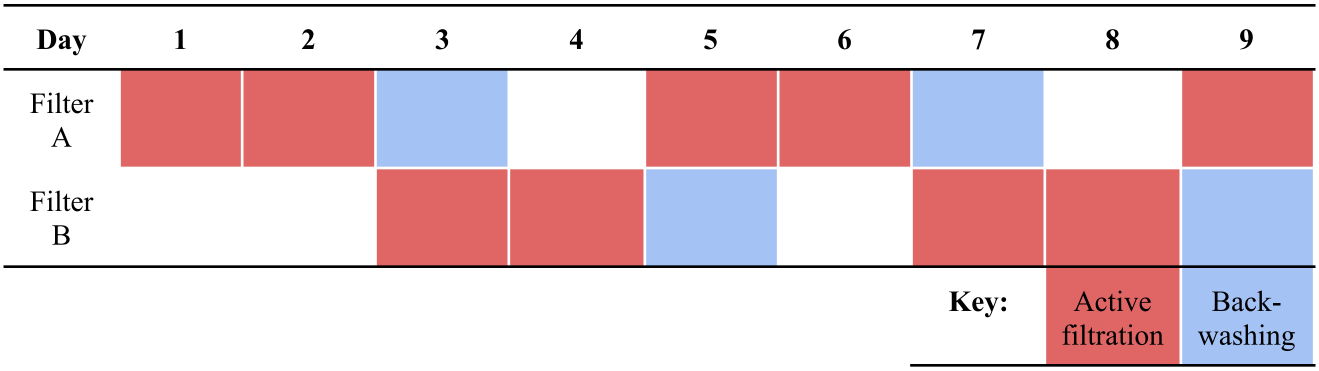

Day	1	2	3	4	5	6	7	8	9
Filter A	🟥	🟥	🟦		🟥	🟥	🟦		🟥
Filter B			🟥	🟥	🟦		🟥	🟥	🟦

Key:	Active filtration	Back-washing
	🟥	🟦

Figure 3.7-1 Depth Filtration Backwashing Schedule

3.7.2 Pressure Drop

Davies' empirical equation (*Equation 3.7-1)* is used for modeling depth filters (Hoppe et al., 2023). The porosity of the cellulose bed is represented by ε, d_f is the fiber diameter, L_f is the filter depth of each subfilter, μ is the dynamic viscosity of water at 35°C, and u is the velocity of the fluid. Based on the calculations performed in *Equation 3.7-1*, a pressure differential of 0.54 bar across the system is required to ensure efficient filtration. To accommodate this pressure loss, the system operates with an inlet pressure of 1.6 bar and an outlet pressure of 1 bar.

$$\textbf{(Eq. 3.7-1)}\ \Delta P = L_f * \left(64\mu u(1 - \varepsilon)^{3/2} \frac{(1+56(1-\varepsilon)^2)}{d_f^{\,2}} \right)$$

Table 3.7-1 Depth Filtration Unit (F-401) Specifications

Parameter	Value
Membrane material	Cellulose
Pore size	0.45 microns
Feed mass flow rate	8,932 kg/hr
System height	1.524 m
System diameter	0.914 m
Recommended backwash flow rate	23,844 kg/hr
Inlet pressure	1.6 bar
Outlet pressure	1 bar
Operating temperature	35°C

3.7.3 Material Balance

The material balance for the system assumes that the entirety of cellular debris is trapped in the filter media and is completely removed during backwashing. A total of 85.4 kg of biomass is captured every hour, as noted by multiplying hourly flow rates in Appendix B. The backwashing with water at a flow rate of 23,844 kg/hr will occur for 30 minutes every 48 hours.

The material balance on cell biomass is as follows:

$$\textbf{(Eq. 3.7-2)}\ M_f * c_f + M_b * c_b = M_w * c_w + M_s * c_s$$

For the purposes of the material balance, the half-hour backwash is averaged over two days, which is equivalent to a flow of 248 kg water/hr. Using *Equation 3.7-2* and the values provided in *Table 3.3-2*, the wastewater flow rate, which consists of water and biomass, was determined to be 339.4 kg/hr.

Table 3.7-2 Depth Filtration Material Balance Specifications

Parameter	Value
Post-fermentation stream flow rate, M_f	8,932 kg/hr
Post-fermentation biomass concentration, c_f	0.0095 kg biomass/kg stream
Backwash water flow rate, M_b	248 kg water/hr*
Backwash water biomass concentration, c_b	0 kg biomass/kg stream
Wastewater flow rate, M_w	339.4 kg/hr
Wastewater biomass concentration, c_w	0.25 kg biomass/kg stream
Filtered stream flow rate, M_s	8,847 kg/hr
Filtered stream flow rate, c_s	0 kg biomass/kg water

Note: *half-hour backwash is averaged over two days.

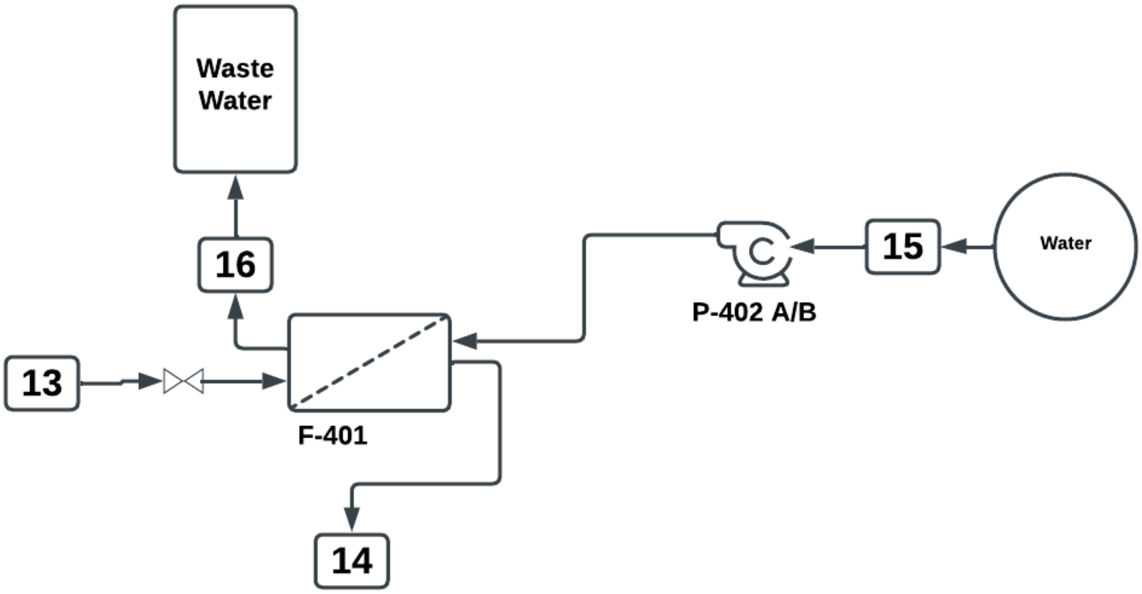

Figure 3.7-2 Depth Filtration System Process Flow Diagram

3.8 Separation System

3.8.1 Unit Design

Distillation is a process well understood and utilized in industry for separations of components based upon boiling point. For this project, a sequence of distillation columns was used to separate the acetone, butanol, ethanol, and water inlet stream into pseudo-pure components. Initial research was conducted into industry standard distillation sequences for ABE fermented products. The most common system was found to be a five column system, as shown in *Figure 3.8-1* (Liu et al., 2022). It aims to strip out each component in different columns ending with a two column decanter system (TCD) to break the water-butanol azeotrope. A second design was compared to one previously described. This distillation sequence differs as it separates the more volatile components from the heavier ones in the second column as seen in *Figure 3.8-2*. The two designs were compared using three different metrics, end product purity, end product extraction rate, and energy efficiency. After simulating both sequences, the second sequence performed better than the first.

Both designs were simulated in Aspen Plus using “RadFrac” blocks as distillation columns. Each column required an upper and lower limit variable to be defined, most often bottom-to-feed ratio and reflux ratio were used. In addition, the theoretical number of stages and theoretical feed stage were manually optimized to reflect the goals defined above. This tedious process required continuous adjustment. If any changes were to occur in preceding columns, the process was repeated to re-optimize subsequent columns. Base operating pressures and temperatures of 1 Bar and 25 °C. The Aspen Plus model outputted theoretical values for number of stages which were translated with a 70% efficiency rate, the model also provided values for column internals such as diameter and column height which are reported in section 6.5.

When initially simulating the processes, the base parameters were mimicked from a previously optimized process (Blignault Van Der Merwe et al., 2010). The design parameters of the columns in this optimized sequence can be found in *Table 3.8-1*. Aspen Further description of other dimensions and internals can be found in section 6.5.

In addition to the 5 distillation columns, a flash and a decanter unit were included in the separation design. A flash unit acts as a separator that takes an inlet and generates a vapor and liquid stream by rapidly reducing pressure or temperature, causing the more volatile components to vaporize. For this project, a flash unit (V-401) was modeled before ultrafiltration (F-401) and serves to model the continual removal of carbon dioxide in fermentation from the post-fermentation product stream (12).

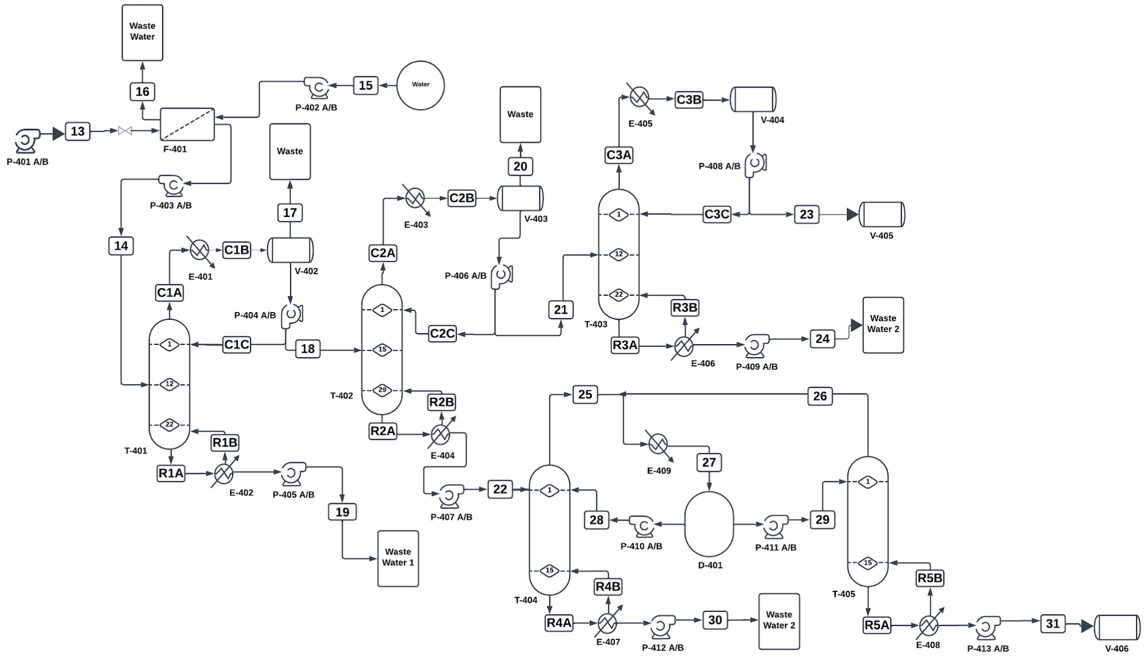

Figure 3.8-3 Final Separations System Process Flow Diagram

Table 3.8-1 Optimized Column Geometry and Stages

Column	Diameter (m)	Actual Stages
Water Column 1 (T-401)	1.83	22
Acetone Column (T-402)	0.61	29
Ethanol Column (T-403)	0.46	22
Water Column 2 (T-404)	0.46	15
Butanol Column (T-405)	0.46	15

The decanter unit serves as a separator that operates on a basis of density. In this specific process, it separates a butanol-water azeotrope into an organic stream and an aqueous stream (streams 29 and 28), which will be fed to the Butanol Column (T-450) and the Water Column 2 (T-440) respectively. Within Aspen Plus, the decanter unit (D-460) was modeled as a Flash 3 unit. Both the temperature and pressure were manually optimized for the greatest amount of butanol and water separations.

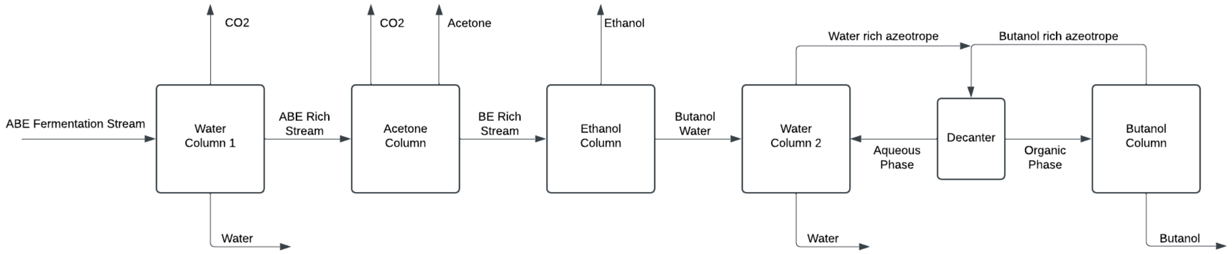

Figure 3.8-1 Block Flow Diagram of Initial 5 Column System

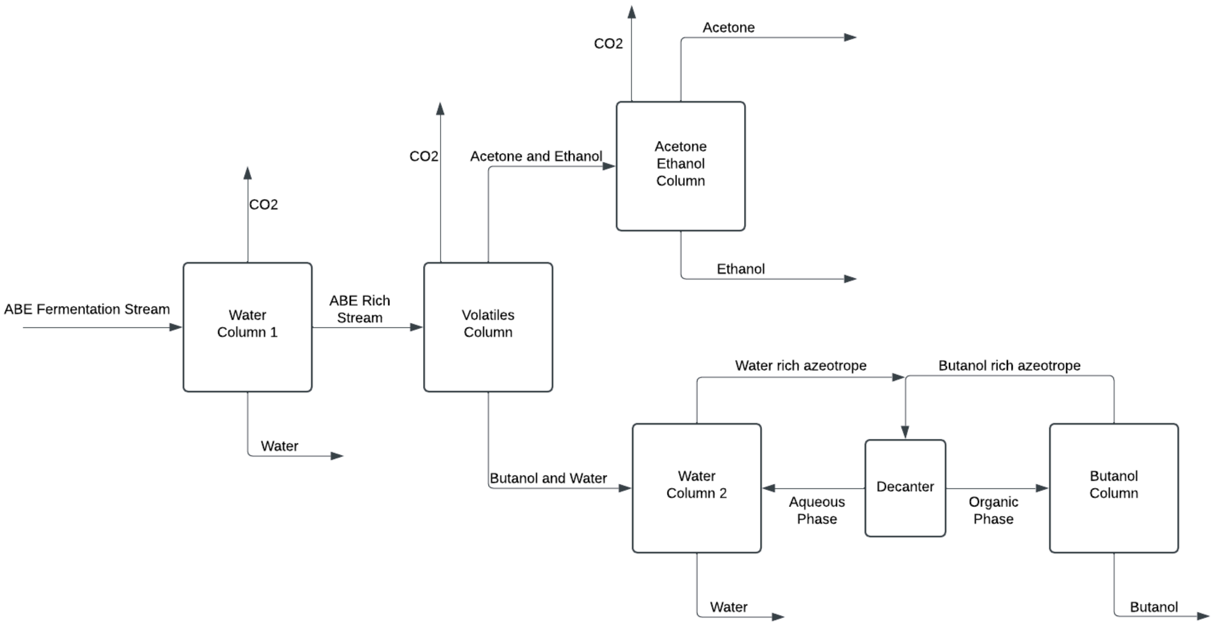

Figure 3.8-2 Block Flow Diagram of Final Distillation Design

3.9 Pumps & Compressor

Pumps facilitate the safe and efficient transfer of materials between processing units while maintaining regulated pressure throughout the system. In the upstream and fermentation section of the process, there are a total of twelve pumps: six primary pumps (P-101, P-102, P-201, P-301, P-302, P-303), each with a designated backup. In the separation portion of the design, fourteen pumps are in service full-time (P-401 through P-414) and fourteen additional pumps are stored as backup.

3.9.1 Pumps & Compressor Design

P-101 moves the starting acid whey feedstock from the storage tank into the ultrafiltration system. Then, P-102 pumps the filtered permeate following ultrafiltration into the reverse osmosis system. C-202 brings atmospheric air into the filtration system before it is used for spray drying. Next, P-301 flows lactose-rich stream leaving the RO system into the fermentation holding tank. Then, P-302 and P-303 flow substrate to the fermenters from the seed train and holding tank, respectively.

In the downstream section following fermentation, there are two pumps (P-401 & P-402) tasked with feeding the fermented substrate into and out of the flash unit. Then, P-403 pumps water to backwash the depth filtration system while P-404 flows the filtered medium out of the system. Within the separation matrix, five pumps serve as reflux pumps (P-405, P-407, P-409, P-411, P-412) and five pumps pump out the bottoms stream (P-406, P-408, P-410, P-413, P-414).

(Eq. 3.9-1) $diff.\ P\ =actual\,P\ +\ total\,frictional\,losses\ +\ \rho_{fluid} * g * h$

Centrifugal pumps are chosen as they standard in industry and can handle high flow rates with ease. All pumps are operated under the assumption that pump efficiency is 70% with a 90% efficient electrical driver. The differential pressure needed to move the fluid from each unit operation is the sum of friction losses in pipes and losses through each heat exchanger, both of which are assumed to be 0.5 bar, one third of the total frictional losses due to control valves, the gravity head, and the actual pressure differential (*Equation 3.9-1)*. P-201 must transport the fluid 10 meters vertically to supply the spray dryer. P-301 must transport the fluid 14 meters vertically to supply to the top of the already raised fermentation tank. The pumps within the separations system must pump to the height of each feed tray. The electric draw for each pump was calculated by dividing the hydraulic power by the product of pump efficiency (70%) and motor efficiency (90%). This accounts for energy losses in both the pump and its electrical driver. These electric draw values are then used to estimate the annual electricity consumption (*Table 4.4-4*) based on pump operating hours, with spare pumps excluded from power calculations. The operating conditions are detailed in *Table 3.9-1*, with summarized conditions provided separately for each process unit in the final recommended design (Section IV).

Table 3.9-1 Pump Operating Conditions

Equipment	Equipment Type	Volumetric Flow Rate (m^3/hr)	Frictional Losses (bar)	Gravity Head (bar)	Differential Pressure (bar)	Hydraulic Power (kW)	Electric Draw (kW)
P-101 A/B	Acid Whey Pumps	27.5	1.35	0	1.95	1.49	2.21
P-102 A/B	Permeate Pumps	25.0	1.35	0	60.4	42.37	62.70
P-201 A/B	Wet Whey Pumps	2.86	0.68	0.78	0	0.17	0.27
P-301 A/B	Storage Pumps	9.58	0.68	1.43	2.1	0.59	0.88
P-302 A/B	Seed Train Pumps	0.009	0.68	0	0.68	0.00017	0.00
P-303 A/B	Fermenter Pumps	10.06	0.68	0	0.68	0.19	0.28
P-401 A/B	Fermentation Product Pumps	9.97	0.68	0	0.68	0.32	0.47
P-402 A/B	Depth Filtration Backwash Pumps	0.21	0.68	0	1.28**	0.004	0.01
P-403 A/B	Post-Depth Filtration Pumps	22.32	0.68	0	1.68	0.42	0.40*
P-404 A/B	Water Column I Reflux Pumps	1.14	1.35	1.1	1.35	0.087	0.13*
P-405 A/B	Water Column I Bottoms Pumps	8.57	1.35	0	1.85	0.05	0.19*
P-406 A/B	Volatiles Column Reflux Pumps	0.10	1.35	1.2	1.35	0.0057	0.01*
P-407 A/B	Volatiles Column Bottoms Pumps	1.11	1.35	0	3.13	0.74	0.09*
P-408 A/B	A & E Column Reflux Pumps	0.07	1.35	1.1	1.35	0.0017	0.00*
P-409 A/B	A & E Column Bottoms Pumps	0.03	1.35	0	1.85	0.008	0.00*
P-410 A/B	Decanter Aqueous Phase Pumps	0.49	1.35	0	3.13	0.38	0.04*
P-411 A/B	Decanter Organic Phase Pumps	0.27	1.35	0	2.54	0.01	0.01*
P-412 A/B	Water Column 2 Bottoms Pumps	0.92	1.35	0	1.85	0.4	0.02*
P-413 A/B	Butanol Column Bottoms Pumps	0.20	1.35	0	1.85	0.005	0.02*

Note: *electric draw values were pulled directly from ASPEN and not estimated from the hydraulic power
**assumed that pressure drop during backwash would be the same as while filtering despite the increased flow rate

A compressor, C-201 is used to bring atmospheric air into the system, through a filter, and into the spray drying apparatus. To determine the characteristics of this compressor, a simulation in Aspen Plus V14 was conducted. The inputs provided to the simulation were the amount of air being moved and the pressure differential.

Table 3.9-2 Compressor Operating Conditions

Equipment	Equipment Type	Inlet Pressure (bar)	Outlet Pressure (bar)	Differential Pressure (bar)	Electric Draw (kW)
C-201	Air Inlet Compressor	1	2	1	904

3.10 Heat Exchangers

Heat exchangers are used to regulate the temperature of fluids, which is critical for units such as the spray dryer and fermentation system, which are designed to operate at specific temperatures.

3.10.1 Pretreatment Heat Exchangers Design

Heat exchangers are critical to our process for heating and cooling process streams efficiently. We designed the heat exchangers using the fundamental energy balance equation (*Equation 3.10-1*) and heat of vaporization equation (*Equation 3.10-2*). Heat capacities of 4.184 and 2.42 kJ/kg•ºC were used for water and pure ethylene glycol, respectively (Engineeringtoolbox, 2025). Since a 50% water and 50% ethylene glycol mixture is used as a coolant in E-102, a heat capacity 3.302 kJ/kg•ºC was used for the mixture. To ensure effective heat transfer, we also applied the heat exchanger design equation (*Equation 3.10-3)*. It is important to note that our design specifications are based on counter-current shell and tube heat exchangers, as modeled in *Figure 3.10-1*.

(Eq. 3.10-1) $Q = mC\Delta T$

(Eq. 3.10-2) $Q = m\Delta H$

(Eq. 3.10-3) $Q = UA\Delta T_{LM}$

$$\text{where } \Delta T_{LM} = \frac{\Delta T_1 - \Delta T_2}{ln(\frac{\Delta T_1}{\Delta T_2})}$$

$$\Delta T_1 = T_{h,in} - T_{c,out}$$

$$\Delta T_2 = T_{h,\, out} - T_{c,\, in}$$

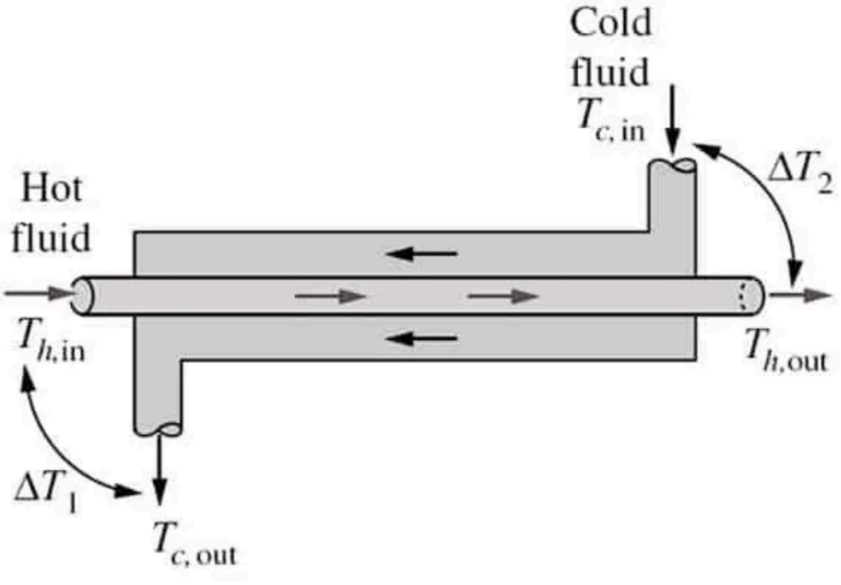

Figure 3.10-1 Counter-Current Heat Exchanger Diagram

Each heat exchanger was designed based on process requirements for heating and cooling specific streams. E-101 heats the acid whey stream using saturated steam, while E-102 removes excess heat from permeate using the ethylene glycol mixture coolant. The air stream and substrate are also heated in E-201 and E-301, respectively, using steam as the heating medium.

The overall heat transfer coefficients and surface areas were selected based on typical values for liquid-liquid and gas-liquid, and gas-gas heat exchangers are 285, 30, and 30 W/m^2K, respectively, ensuring efficient thermal exchange while maintaining feasible equipment sizing

(Peters, Timmerhaus, & West, 2003). The heat exchanger duties were calculated based on the process conditions, with variables and results summarized in *Table 3.10-1* and *Table 3.10-2*.

Table 3.10-1 Pretreatment Heat Exchanger Operating Conditions

Equipment ID	Equipment Type	Stream of Interest	Flow Rate (kg/hr)	Stream Temperatures (^oC)	
				Inlet	Outlet
E-101	Acid whey heater	Acid whey	27,215	25	48
		Saturated steam at 1 bar	916	120	120
E-102	Permeate cooler	Permeate	24,962	48	25
		Ethylene glycol mixture	756	5	15
E-201	Air stream heater	Air	33,984	25	180
		Saturated steam at 10 bar	5,602	250	250
E-301	Substrate Heater	Sugar solution	10,854	25	35
		Saturated steam at 1 bar	192	120	120

Table 3.10-2 Pretreatment Heat Exchanger Design Parameters

Equipment ID	Equipment Type	Overall Heat Transfer Coefficient (W/m^2)	Surface Area (m^2)	Duty (kW)
E-101	Acid whey heater	30	312	735
E-102	Permeate cooler	285	90.2	-667
E-201	Air stream heater	30	459	1471
E-301	Substrate heater	30	44.7	120.6

3.10.2 Fermenter Heat Exchangers Design

In each of the ten fermentation reactors, heat must be efficiently removed to maintain an optimal operating temperature of 35°C. The total heat generation per reactor is determined by the sum of the heat from agitation and the heat from the biological reaction. The power input from agitation is calculated using the relationship between impeller characteristics and fluid properties seen in Eq. 3.10-3. The metabolic heat generation, on the other hand, is driven by substrate consumption and the associated heat yield coefficient. Eq. 3.10-4 defines the relationship between heat release and substrate metabolism.

(Eq. 3.10-4) $$P_{agitation} = N_p \rho n^3 D^5$$

(Eq. 3.10-5) $$Q_{reaction} = Y_Q r_{substrate} V$$

The associated variables and their respective values are outlined in *Table 3.10-3*. The substrate consumption rate is 2.62 g/(L·hr), representing the average rate at which substrate is metabolized during fermentation. This was calculated by dividing the total change in substrate concentration—from 99.5 g/L initially to 0 g/L at the end—by the total fermentation time of 38 hours. Additionally, the heat yield coefficient, given as 20 kJ/g, defines the amount of heat released per gram of substrate consumed. When combined with the substrate consumption rate and total fermentation volume, this value allows for the estimation of the total heat load generated by microbial metabolism, which is critical for designing an appropriate cooling system.

Table 3.10-3 Fermentation Energy Balance Variables

Variable	Value
Power Number (N_P)	5.5
Broth Density (ρ)	1,042 kg/m^3
Impeller RPM (n)	100 rpm
Impeller Diameter (D)	1.2 m
Heat Yield Coefficient (Y_Q)	20 kJ/g
Substrate Consumption Rate ($r_{substrate}$)	2.62 g/(L·hr)
Total Fermentation Volume (V)	500,000 L

Note. N_P from Chapple et al. (2002); ρ from McDonald & Turcotte (1948); Y_Q from Ghaly et al. (2005).

The total heat generated from agitation in the 10 reactors was calculated to be 0.066 MW. Likewise, the total heat generated from fermentation sum to 7.278 MW. Thus, 0.734 MW of cooling capacity per reactor is required to maintain a reactor temperature of 35°C.

To achieve this cooling requirement, each reactor is connected to an external heat exchanger that utilizes cooling water at a flow rate of 50 m^3/h. Using external heat exchangers instead of relying solely on reactor jackets is a common practice in large-scale ABE fermentation systems (Alfalaval, 2025). This setup ensures that the heat generated is rapidly transferred away from the fermentation broth, preventing excessive temperature fluctuations that could negatively impact microbial activity and product yields. The required heat transfer area for each exchanger is 659 m^2, which allows for efficient heat removal and ensures that the fermentation process remains stable and controlled. This area is split between the cooling jacket and external heating exchanger, with a minimum temperature difference of 1°C taken in both. The heat exchanger specifications and parameters are outlined in *Table 3.10-4* and *Table 3.10-5*.

Table 3.10-4 Fermenter Heat Exchanger Operating Conditions

Equipment ID	Equipment Type	Stream of Interest	Flow Rate (kg/hr)	Stream Temperatures (ºC)	
				Inlet	Outlet
R-302 - R-311	Fermenter	Reactor Content	-	35	35
		Cooling Water at 1 bar	50,000	25	34

Table 3.10-5 Fermentation Heat Exchanger Design Parameters

Equipment ID	Equipment Type	Overall Heat Transfer Coefficient (W/m^2)	Surface Area (m^2)	Total Duty (kW)
R-302 - R-311	Cooling Jacket	285	83	93
E-302 - E-311	External Heat Exchanger	285	573	641

3.10.3 Separations Heat Exchangers Design

Throughout the separations process there are a number of heat exchangers. Most of these are overhead condensers and reboilers associated with the different distillation columns. All heat exchangers within the separation blocks were modeled in Aspen Plus V14 and their specifications and parameters are outlined in *Table 3.10-6* and *Table 3.10-7*.

Table 3.10-6 Separations Heat Exchanger Operating Conditions

Equipment ID	Equipment Type	Stream of Interest	Flow Rate (kg/hr)	Stream Temperatures (ºC)	
				Inlet	Outlet
E-401	Water Column I Condenser	Water Column I Distillate	1,087	110	35
		Liquid Water at 1 bar	7,612	25	35
E-402	Water Column I Reboiler	Water Column I Bottoms	7,757	112	112
		Steam at 7 bar	3,894	170	170
E-403	Volatiles Column Condenser	Volatiles Column Distillate	80	71	35
		Liquid Water at 1 bar	249	25	35
E-404	Volatiles Column Reboiler	Volatiles Column Bottoms	995	91	91
		Steam at 7 bar	860	170	170
E-405	Acetone Ethanol Column Condenser	AE Column Distillate	54	56	35
		Liquid Water at 1 bar	55	25	35
E-406	Acetone Ethanol Column Reboiler	AE Column Bottoms	26	81	81
		Steam at 7 bar	312	170	170
E-407	Water Column II Reboiler	Water Column II Bottoms	846	100	100
		Steam at 7 bar	553	170	170
E-408	Butanol Column Reboiler	Butanol Bottoms	149	93	99
		Steam at 7 bar	73	170	170
E-409	Azeotrope Condenser	Mixed Azeotrope Stream	694	95	35
		Liquid Water at 1 bar	1,685	25	35

Table 3.10-7 Separations Heat Exchanger Design Parameters

Equipment ID	Equipment Type	Surface Area (m^2)	Total Duty (kW)
E-401	Overhead Condenser 1	218	-7,347
E-402	Column 1 Reboiler	140	8,036
E-403	Overhead Condenser 2	31	-428
E-404	Column 2 Reboiler	77	493
E-405	Overhead Condenser 3	17	-178
E-406	Column 3 Reboiler	2.7	179
E-407	Column 4 Reboiler	4.5	317
E-408	Column 5 Reboiler	1	42
E-409	Azeotrope Condenser	11	-185

Note. Heat Transfer Coefficient is not reported for these heat exchangers due to Aspen supplying them.

IV. ECONOMICS

4.1 Operating Schedule

When evaluating the economics of this process design, it is important to consider not only the annual revenues and operating costs, but also the full project timeline, including construction and operating phases. The proposed schedule begins with a 18-month construction period, during which all equipment and infrastructure are installed and commissioned. This is followed by a 6-month ramp-up phase where the facility operates at 50% capacity, allowing time for operator training, troubleshooting, and system optimization. After this initial phase, the plant is expected to run at full capacity for 20 years, forming the basis of long-term financial projections.

The facility is designed to operate 330 days per year, allowing time for planned downtime and maintenance. This schedule accounts for federal holidays and inevitable production losses due to start-up and shutdown procedures. Additionally, a multi-week shutdown period at the end of each year is built into the schedule to allow for thorough cleaning, equipment audits, disassembly, and refurbishing. These measures ensure continued safe, efficient, and compliant operations throughout the plant's life cycle. Within this broader operating schedule, the fermentation reactors run on a 48-hour batch cycle, with each reactor completing one batch every two days, as previously mentioned in *Table 3.5-4*.

4.2 Annual Revenue

Estimated annual revenue for the process is approximately $98 million, as shown in *Table 4.2-1*. The vast majority of this revenue (98%) is generated from the sale of whey protein, which is priced at $12.00/kg and produced in large quantities (over 8 million kg/year). This pricing was conservatively estimated based on a review of commercial listings for whey protein concentrate, which typically range from \$18 to \$22 per kilogram in post-packaging retail and small-batch bulk markets. Because our process outputs unbranded, unpackaged protein sold directly to packagers, we inferred a lower, pre-packaging wholesale price. A working estimate of \$12.00/kg was chosen to reflect this earlier point in the value chain while remaining within a commercially plausible range. In contrast, revenue from butanol and acetone is significantly smaller, totaling about \$1.38 million and \$478,000 per year, respectively. Given this distribution, the overall revenue is highly sensitive to fluctuations in the market price or purity requirements of whey protein. Any disruptions in protein yield, quality, or price could significantly impact the financial performance of the process.

Table 4.2-1 Estimated Annual Revenue

Component	Amount (kg/year)	Unit Price (\$/kg)	Revenue (\$/yr)
Acetone	362,010	1.32	477,853
Butanol	1,077,285	1.28	1,378,925
Whey Protein	8,015,040	12.00	96,180,480
		Total Revenue (\$/year)	**98,037,258**

4.3 Purchased Equipment and Capital Costs

A key factor in evaluating the project's economic feasibility is the capital investment needed for equipment purchases. These costs are divided into two categories: major equipment costs, outlined in *Table 4.3-1*, and ancillary equipment costs, shown in *Table 4.3-2*. In cases where vendor pricing was unavailable, pricing was determined via cost correlation graphs (Peters, Timmerhaus, & West, 2003), using *Equation 4.3-1* (Towler & Sinnott, 2022), or via Aspen Plus simulation data. In this equation, a, b, and n are constants specific to the equipment type, and S represents a size parameter, with the equation being valid only within defined size limits. For the purposes of this analysis, it is important to note that this correlation was used outside of the size limitations for the pumps, as the pumps in this project are very large.

$$\textbf{(Eq. 4.3-1)}\ C_e = a + bS^n$$

$$\textbf{(Eq. 4.3-2)}\ C = C_e * \frac{(current\ CEPCI)}{2007\ CEPCI}$$

It is important to highlight that cost estimates derived from *Equation 5.1-1* do not account for inflation, as the original formulation reflects pricing as of January 2007 (Towler & Sinnott, 2022). To adjust for this, the equation was modified using a Chemical Engineering Plant Cost Index (CEPCI) correction factor, where a current CEPCI value of 800 was divided by 509.7, the January 2007 CEPCI reported by Towler and Sinnott.

4.3.1 Major Equipment

Major equipment was priced using one of the strategies described above. Each piece of equipment was designed to safely operate within the expected temperature and pressure ranges. A summary of these costs is provided in *Table 4.3-1*.

Table 4.3-1 Summary of Major Equipment Purchased

Unit ID	Unit Name	Purchased Cost
Pre-Treatment		**$2,314,689**
F-101	Ultrafiltration System	$1,040
F-201	Air Filter	$1,599
H-201	Spray Dryer	$2,308,300
RO-101 + RO-102	Reverse Osmosis System	$3,750
Fermentation		**$12,848,652**
R-301	C. *acetobutylicum* Seed Train Unit	$219,722
R-302	Batch ABE Fermentation Reactor	$1,262,893
R-303	Batch ABE Fermentation Reactor	$1,262,893
R-304	Batch ABE Fermentation Reactor	$1,262,893
R-305	Batch ABE Fermentation Reactor	$1,262,893
R-306	Batch ABE Fermentation Reactor	$1,262,893
R-307	Batch ABE Fermentation Reactor	$1,262,893
R-308	Batch ABE Fermentation Reactor	$1,262,893
R-309	Batch ABE Fermentation Reactor	$1,262,893
R-310	Batch ABE Fermentation Reactor	$1,262,893
R-311	Batch ABE Fermentation Reactor	$1,262,893
Distillation		**$1,180,451**
T-401	Water Column I	$521,900
T-402	Volatiles Column	$245,600
T-403	Acetone Ethanol Column	$71,200
T-404	Water Column II	$174,700
T-405	Butanol Column	$46,500
F-401	Depth Filtration System	$9,451
V-402	Water Column I Reflux Drum	$34,600
V-403	Volatiles Column Reflux Drum	$18,400
V-404	Acetone Ethanol Column Reflux Drum	$22,000
D-401	Decanter	$36,100
	Total Cost	**$16,343,792**

4.3.2 Ancillary Equipment

Ancillary equipment was priced using one of the strategies described above. Each piece of equipment was designed to safely operate within the expected temperature and pressure ranges. A summary of these costs is provided in *Table 4.3-2*.

Table 4.3-2 Summary of Ancillary Equipment Purchased

Unit ID	Unit Name	Purchased Cost
Pre-Treatment Heat Exchangers/Storage		**$828,846**
V-101	Acid Whey Storage Vessel	$0
V-201	Whey Protein Product Storage	$177,846
E-101	Acid Whey Preheater	$42,000
E-102	Permeate Cooling	$9,000
E-201	Air Stream Heater	$600,000
Fermentation Heat Exchangers/Storage		**$1,051,849**
V-301	Concentrate Permeate Storage	$261,849
E-301	Substrate Heater	$10,000
E-302	Fermentation Tank Cooler	$78,000
E-303	Fermentation Tank Cooler	$78,000
E-304	Fermentation Tank Cooler	$78,000
E-305	Fermentation Tank Cooler	$78,000
E-306	Fermentation Tank Cooler	$78,000
E-307	Fermentation Tank Cooler	$78,000
E-308	Fermentation Tank Cooler	$78,000
E-309	Fermentation Tank Cooler	$78,000
E-310	Fermentation Tank Cooler	$78,000
E-311	Fermentation Tank Cooler	$78,000
Distillation Heat Exchangers		**$768,400**
E-401	Water Column I Condenser	$253,000
E-402	Water Column I Reboiler	$363,600
E-403	Volatiles Column Condenser	$37,300
E-404	Volatiles Column Reboiler	$25,100
E-405	Acetone Ethanol Column Condenser	$13,700
E-406	Acetone Ethanol Column Reboiler	$15,200
E-407	Water Column II Reboiler	$29,400
E-408	Butanol Column Reboiler	$16,400
E-409	Azeotrope Condenser	$14,700
Pre-Treatment Pumps		**$2,808,832**
C-202	Air Stream Compressor	$2,735,600
P-101 A/B	Acid Whey Pumps	$25,690
P-102 A/B	Permeate Pumps	$25,358

P-201 A/B	Wet Whey Pumps	$22,184
Fermentation Pumps		**$68,158**
P-301 A/B	Storage Pumps	$23,218
P-302 A/B	Seed Train Pumps	$21,663
P-303 A/B	Fermenter Pumps	$23,277
Distillation Pumps		**$190,194**
P-401 A/B	Fermented Stream Pumps	$23,276
P-402 A/B	Depth Filtration Backwash Pumps	$21,718
P-403 A/B	Post-Depth Filtration Pumps	$12,400
P-404 A/B	Water Column I Reflux Pumps	$29,200
P-405 A/B	Water Column I Bottoms Pumps	$10,600
P-406 A/B	Volatiles Column Reflux Pumps	$13,800
P-407 A/B	Volatiles Column Bottoms Pumps	$12,400
P-408 A/B	Acetone Ethanol Column Reflux Pumps	$12,000
P-409 A/B	Acetone Ethanol Column Bottoms Pumps	$10,600
P-410 A/B	Decanter Aqueous Phase Pump	$10,600
P-411 A/B	Decanter Organic Phase Pump	$10,600
P-412 A/B	Water Column 2 Bottoms Pumps	$12,400
P-413 A/B	Butanol Column Bottoms Pumps	$10,600
Distillation Product Storage		**$27,638**
V-405	Acetone Product Storage	$13,819
V-406	Butanol Product Storage	$13,819
	Total Cost	**$5,743,917**

4.3.3 Total Capital Cost of Plant

To estimate the total installed capital cost for our solid-fluid processing facility, we applied a Lang factor—a widely used heuristic in process design that relates total fixed capital cost to purchased equipment cost. The Lang factor accounts for additional costs such as installation, piping, electrical, instrumentation, and civil work. A Lang Factor of 3.63 was chosen according to recommendations for a solid and liquids processing plant (Towler & Sinnott, 2022). By multiplying our base equipment cost of $22 million by 3.63, we arrived at a total capital cost estimate of around \$80 million. Details can be found in *Table 4.3-3*. It is important to note that the land cost of \$825,000 was excluded from this multiplication, as it is not subject to installation or construction-related expenses covered by the Lang factor.

Table 4.3-3 Total Capital Cost of Plant with Lang Factor Calculation

Section	Purchased Costs	Overall Capital Costs
Upstream Major Equipment	\$2,314,689	\$8,402,320
Upstream Ancillary Equipment	\$3,637,678	\$13,204,771
Fermentation Major Equipment	\$12,848,652	\$46,640,607
Fermentation Ancillary Equipment	\$1,120,007	\$4,065,624
Separation Major Equipment	\$1,180,451	\$4,285,037
Separation Ancillary Equipment	\$987,794	\$3,585,692
Subtotal	**\$22,089,270**	**\$80,184,051**
Land	\$825,000	\$825,000
Total	**\$22,914,270**	**\$81,009,051**

4.4 Operating Costs

The evaluation of operating costs is a critical component of the overall economic assessment of the process design. Operating costs encompass the recurring expenses associated with the day-to-day operation and maintenance of the facility, directly influencing the profitability and long-term viability of the project. These costs, for the purpose of this discussion, include raw material procurement, utilities, labor, waste treatment. By systematically estimating these expenditures, this section aims to present a clear and detailed account of the operational expenditures, supporting an informed analysis of the process economics.

4.4.1 Raw Materials

The acid whey feedstock used in this process is sourced as a byproduct from the Chobani facility in Twin Falls, Idaho. Since Chobani would otherwise incur costs to dispose of this waste stream, the feedstock is provided at no charge, resulting in zero raw material cost for the process (*Table 4.4-1*).

As a result, our gross margin is effectively our revenue, since raw material costs are negligible and gross margin is the difference between revenue and raw material costs.

Table 4.4-1 Raw Material Operating Costs

Component	Amount (kg/year)	Unit Cost ($/kg)	Cost ($/year)
Acid Whey Feedstock	215,546,950	0.00	0
		Total Cost ($/year)	**0**

4.4.2 Labor Costs

Labor costs are a major component of overall operating expenses, primarily driven by the number of operators required to staff the facility continuously. As shown in *Table 4.4-2*, the total labor cost is estimated at $9,860,000 per year, which includes salaries for approximately 135 operators, 2 lead engineers, and 1 plant manager. Operator salaries are set at $70,000 annually, while lead engineers and the plant manager earn $130,000 and $150,000 per year, respectively.

The number of operators per shift was estimated using the method provided by the textbook A*nalysis, Synthesis, and Design of Chemical Processes*, which employs *Equation 4.4-1*, where N_{ol} is the operators required per shift, P is the number of operating steps that handle solids, and N_{mp} is the number of major pieces of equipment (Turton et al, 2012). The steps that operate with solids (where P = 1) are Ultrafiltration, Spray Dryer, and Distillation.

$$\textbf{(Eq. 4.4-1)}\ N_{ol} = (6.29 + 31.7P^2 + 0.23N_{mp})^{1/2}$$

This formula helps estimate staffing needs for a 24/7 operation. With 5 shifts needed to ensure around-the-clock coverage for 330 days per year, the total number of operators per equipment block was scaled accordingly. For example, ultrafiltration, spray drying, and distillation each required 7 operators per shift, resulting in 35 operators per area. These labor estimates ensure safe and continuous operation across all critical unit operations. It is important to note that this is a conservative approximation and in practice, less operators may be required as operators can work on multiple pieces of equipment.

Table 4.4-2 Labor Operating Costs

Block	Major Equipment	Operators per Shift	Number of Operators
Ultrafiltration	F-101	7	35
RO System	RO-101, RO-102	3	15
Spray Dryer	H-201	7	35
Fermenters	R-301, R-302, R-303, R-304, R-305, R-306, R-307, R-308, R-309, R-310, R-311	3	15
Distillation	F-401, T-401, T-402, T-403, T-404, T-405, D-401	7	35
		Total Operators	135
		Operator Salary (x135)	$70,000
		Lead Engineer Salaries (x2)	$130,000
		Plant Manager Salary (x1)	$150,000
		Total Labor Cost	$9,860,000

4.4.3 Utility Costs

The next major component of operating costs is utility consumption. As shown in Table 4.4-3, total utility operating costs amount to approximately $3.6 million per year. The largest contributor is high-pressure steam (10 bar) at roughly $1.80 million. 1 bar steam costs around $350,000 annually. 7 bar steam used in the distillation matrix constitutes around $5,000 in annual costs. Cooling water, despite its low unit cost of $0.00014/kg, accounts for around $750,000 per year due to its high volumetric use. Electricity contributes $574,000 annually, while ethylene glycol, though used in smaller quantities, adds $140,000 to the yearly costs due to its unit price of \$0.05/kg. These utility expenses are critical for meeting the process's energy and thermal requirements and represent a significant portion of the overall operating budget.

Table 4.4-3 Utility Operating Costs

Component	Amount	UNIT	Unit Cost	UNIT	Cost (\$/year)
Electricity	9,566,412	kWh/year	\$0.06000	\$/kWh	\$573,985
Cooling Water	5,390,318,493	kg/year	\$0.00014	\$/kg	\$754,645
Steam (1 bar)	8,775,360	kg/year	\$0.04010	\$/kg	\$351,892
Steam (7 bar)	118,237	kg/year	\$0.04025	\$/kg	\$4,759
Steam (10 bar)	44,367,840	kg/year	\$0.04050	\$/kg	\$1,796,898
Ethylene Glycol	2,993,760	kg/year	\$0.04660	\$/kg	\$139,509
				Total Cost (\$/year)	\$3,621,687

Note. Unit Cost of Electricity, Cooling Water, and Steam (1 bar and 10 bar) from Turton et al. (2012); Unit Cost of Ethylene Glycol, Peters, Timmerhaus, and West (2003).

The electricity component of the utility operating costs is broken down in *Table 4.4-4*, which details the electrical usage and cost contributions from various plant equipment. The total annual electricity cost of \$574,000 is primarily driven by electric draws from pumps, distillation units, and agitators. Among these, the compressor, C-202, is the most energy-intensive, consuming nearly 8 million kWh per year and accounting for approximately \$473,000 in annual cost. Other pumps such as P-102 and P-401 also contribute significantly. Additionally, the distillation section and reactor agitators add to the total electricity demand. These components collectively represent the electrical energy needed to operate the plant's fluid transport and separation processes.

Table 4.4-4 Electricity Operating Costs

Equipment	Usage (kWh/year)	Cost ($/year)
Pumps	**538,441**	**32,300**
P-101	17,503	1,050
P-102	496,584	29,800
P-201	2,138	128
P-301	6,970	418
P-302	2	0
P-303	2,218	133
P-401	1,980	119
P-402	3,722	223
P-403	55	3
P-404	3,196	192
P-405	1,030	62
P-406	1,516	91
P-407	63	4
P-408	688	41
P-409	24	1
P-410	6	0
P-411	307	18
P-412	113	7
P-413	163	10
P-414	163	10
Miscellaneous	**9,028,404**	**542,000**
C-201	7,888,320	473,000
H-201	264,000	15,800
Distillation	462,132	27,700
R-301 - R-310	413,952	24,800
Total	**9,566,844**	**574,000**

4.4.4 Waste Disposal Costs

An additional component of operating costs includes waste disposal expenses, which account for the removal of various byproducts and residuals generated throughout the process.

As shown in *Table 4.4-5*, total annual waste disposal costs are relatively low, amounting to around $10,542. The majority of this cost comes from disposing of large quantities of water, which contributes $10,491 per year, due to its high volume despite a minimal unit cost. Other waste streams such as butanol, ethanol, acetic acid, butyric acid, and *Clostridium acetobutylicum* add marginal costs. According to Turton et al. and *Table 8.3*, the unit cost of waste treatment is based on the price for tertiary treatment—$56 per 1,000 m^3—which includes filtration, activated sludge processing, and chemical treatment (Turton et al., 2012). Most of our organic wastes are solvated in water, therefore the costs associated with disposing of this waste is the cost for tertiary wastewater treatment. Certain components like acetone and carbon dioxide are vented into the atmosphere. The cost for vented treatment was decided to be $0, this could be further researched based upon the location of our plant and a price per kg could be associated with this vented stream (*Table 4.4-6*).

Table 4.4-5 Waste Water Disposal Costs

Component	Amount (kg/year)	Unit Cost $/kg	Cost ($/year)
Water	**187,347,600**	$0.000056	$10,491
Acetone	**7,920**	$0.000056	$0
Butanol	**31,680**	$0.000056	$2
Ethanol	**102,960**	$0.000056	$6
Acetic Acid	**23,760**	$0.000056	$1
Butyric Acid	**63,360**	$0.000056	$4
C. acetobutylicum	**673,200**	$0.000056	$38
		Total Cost ($/year)	**$10,542**

Table 4.4-6 Off-Gas Disposal Costs

Component	Amount (kg/year)	Unit Cost ($/kg)	Cost ($/year)
Acetone	23,760	$0	$0
Carbon Dioxide	2,138,400	$0	$0
		Total Cost ($/year)	**$0**

4.5 Cost of Manufacturing

Before assessing the economic feasibility of a chemical process, it is necessary to estimate the cost of manufacturing (COM)—the recurring expenses associated with operating a chemical plant. Unlike capital costs, which are one-time expenditures, manufacturing costs are expressed in dollars per unit time and account for direct operating expenses, fixed charges, and general overhead. Direct costs include variable expenses such as utilities, waste treatment, and operating labor—many of which are estimated based on operating conditions and are directly tied to production rate. Fixed costs, such as depreciation, insurance, and overhead, are independent of production rate and are typically estimated as percentages of the Fixed Capital Investment (FCI) or labor cost. General expenses cover business-related costs such as administration, distribution, and R&D, and are usually calculated as fractions of COM, labor, or FCI.

The COM depends on inputs such as the fixed capital investment (FCI), operating labor, utilities, waste treatment, and raw materials, which can often be estimated from process flow diagrams and early design data. The cost of manufacturing (COM) can be determined when the following cost components are known or can be reasonably estimated: fixed capital investment (FCI), cost of operating labor (C_{OL}), cost of utilities (C_{UT}), cost of waste treatment (C_{WT}), and cost of raw materials (C_{RM}). The FCI in this case was taken to be the total capital costs calculated in Section 4.3.3. Based on this, the COM was calculated using *Equation 4.5-1* using values detailed in *Table 4.5-1*. A further breakdown of the estimated manufacturing costs is outlined in *Table 4.5-2*.

(Eq. 4.5-1) $COM = 0.280FCI + 2.73C_{OL} + 1.23(C_{UT} + C_{WT} + C_{RM})$

Table 4.5-1 Cost of Manufacturing Summary

Variable	Value
Fixed Capital Investment (FCI)	\$81,009,051
Cost of Labor (C_{OL})	\$9,860,000
Cost of Utilities (C_{UT})	\$3,621,687
Cost of Waste Treatment (C_{WT})	\$10,520
Cost of Raw Materials (C_{RM})	\$0
Cost of Manufacturing (COM) (\$/year)	**\$54,067,949**

Table 4.5-2 Cost of Manufacturing Summary

Category	Estimation	Annual Cost ($/year)
Direct Costs		**$24,000,000**
Raw Materials	C_{RM}	$0
Waste Treatment	C_{WT}	$10,500
Utilities	C_{UT}	$3,620,000
Operating Labor	C_{OL}	$9,860,000
Direct Supervisory and Clerical Labor	$0.18C_{OL}$	$1,770,000
Maintenance and Repairs	0.06FCI	$4,860,000
Operating Supplies	0.009FCI	$729,000
Laboratory Charges	$0.15C_{OL}$	$1,480,000
Patents and Royalties	0.03COM	$1,620,000
Fixed Costs		**$12,500,000**
Depreciation	0.1FCI	$8,100,000
Local Taxes and Insurance	0.032FCI	$2,590,000
Plant Overhead Costs	$0.708C_{OL} + 0.036FCI$	$9,900,000
General Costs		**$11,100,000**
Administration Costs	$0.177C_{OL} + 0.009FCI$	$2,470,000
Distribution and Selling Costs	0.11COM	$5,950,000
Research and Development	0.05COM	$2,700,000
	Annual COM ($/year):	**$47,600,000**
	COM + Depreciation:	**$55,700,000**

4.6 Cash Flow Analysis

To evaluate the economic viability of the process, we conducted a year-by-year Discounted Cash Flow (DCF) analysis over a 22-year period, consisting of 18 months of construction, a 6-month ramp-up phase at 50% capacity, and 20 years of full-capacity operation. The Fixed Capital Investment (FCI) was evenly distributed across the construction timeline. During the ramp-up phase, cash flows were estimated as half the full-capacity revenue and half the full-capacity cost of manufacturing, while maintaining full labor costs.

We incorporated depreciation into our analysis using a 10-year straight-line schedule, which allowed for annual depreciation deductions against taxable income starting at the onset of operation. A 10% discount rate was applied to all cash flows, except for the cost of land, to reflect the time value of money. No income taxes were assessed during the construction phase, as the project did not generate positive earnings. Once the facility began turning a profit, Idaho's corporate income tax was applied at 5.695%, as well as a flat 21% federal income tax rate (Tax Foundation, 2025). We also computed the cumulative DCF across all years to better understand long-term project performance and breakeven timing.

The individual monthly discounted cash flow (DCF) profile illustrates the project's cash flow dynamics over its entire life cycle and can be seen in *Figure 4.6-1*. During the initial construction phase, which spans approximately the first 18 months, the project incurs significant negative cash flows due to substantial capital expenditures. Following this period, the project begins to generate positive cash flows as operations commence. The magnitude of positive cash flows increases initially as the facility ramps up production, after which the discounted cash flows gradually decline over time. Overall, the figure demonstrates that while the early years are capital-intensive, the project achieves consistent positive returns once operational, contributing to the long-term cumulative profitability.

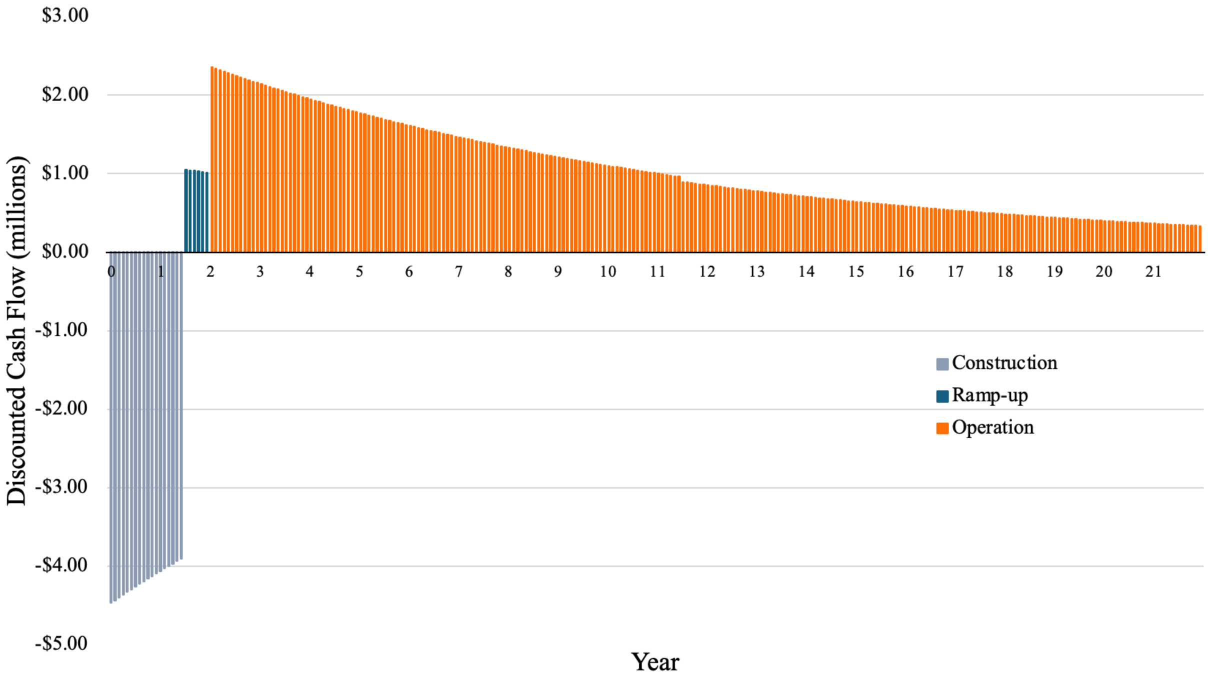

Figure 4.6-1 Individual Discounted Cash Flow Diagram

The cumulative DCF profile (*Figure 4.6-2*) illustrates the project's overall recovery of investment and profitability over its operational life. During the initial construction phase, cumulative DCF declines as capital expenditures are incurred. After operations commence, positive cash flows gradually accumulate, and the project reaches its breakeven point — where cumulative discounted inflows equal the initial investment — after approximately 4.5 years. Beyond this point, the project continues to generate steady positive cash flow, resulting in sustained growth in cumulative DCF over the remaining life of the facility.

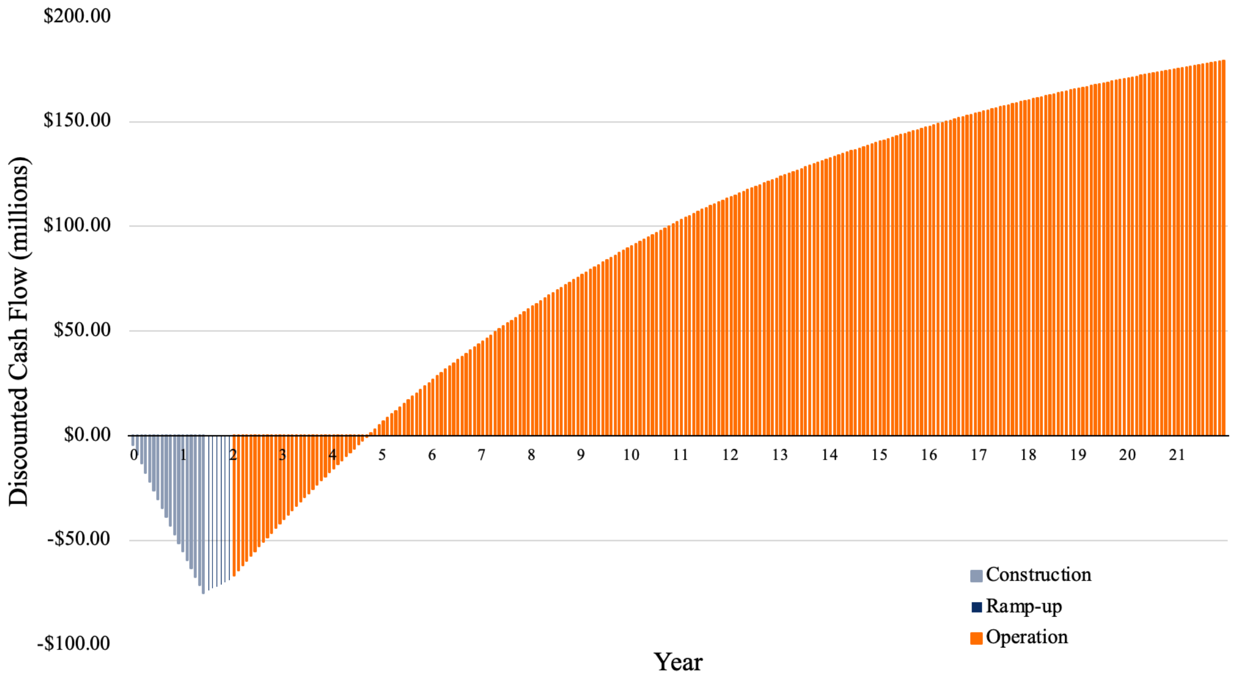

Figure 4.6-2 Cumulative Discounted Cash Flow Diagram

The economic evaluation of the project reveals a significant contrast between the calculated return on investment (ROI) and the internal rate of return (IRR). The total after-tax ROI is approximately 731%, indicating that over the full operational life of the facility, the project is expected to generate nearly ten times its initial capital investment in cumulative after-tax cash flow. However, the IRR is relatively modest at around 35.76%, reflecting the extended timeline of the project and the gradual accumulation of profits over time. This discrepancy arises because ROI captures the total return without considering the time value of money, whereas IRR accounts for the timing of cash inflows and penalizes cash flows that occur later in the project life. In this case, the initial investment is substantial and heavily front-loaded, while positive cash flows only begin after an extended construction period and are distributed over more than 20 years of operation. As a result, while the project demonstrates strong overall profitability, the low IRR suggests a lower annualized efficiency of capital use, which may be less attractive to investors seeking quicker returns.

4.7 Scenarios

It is important to analyze specific circumstances and design choices that could contribute to improving the overall profitability of the process. In this analysis, two scenarios were explored to identify opportunities for improving the profitability of the process design. First, the potential impact of a sustainability tax credit was considered, which would directly enhance the project's after-tax cash flows and improve both ROI and IRR. Second, the economic performance of the process was evaluated focusing solely on the production of whey protein, which represents the primary revenue driver for the facility. These scenarios highlight how strategic design and policy incentives can materially influence the project's financial viability.

4.7.1 Scenario 1: $0.70 Sustainability Tax Credit

Scenario 1 considers the potential impact of a $0.70 per kilogram tax credit applied to the renewable biobutanol produced in the process, modeled after existing U.S. federal biofuel incentives such as those found in the Renewable Fuel Standard (RFS) and the Inflation Reduction Act (IRA). In the U.S., biofuel tax credits are a central policy tool used to accelerate the transition to low-carbon fuels. These credits are often structured as volumetric or mass-based incentives (e.g., $/gal or $/kg) and are tied to lifecycle greenhouse gas reductions. Notable examples include the Biodiesel Tax Credit and the new Clean Fuel Production Credit (Section 45Z), which rewards low-carbon fuel producers based on carbon intensity metrics.

For this project, a $0.70/kg credit on biobutanol would provide a substantial supplemental revenue stream linked directly to the fuel's environmental value. While the project does not currently qualify for such a credit, modeling its impact shows a clear improvement in financial metrics, raising both ROI and IRR, and underscores the importance of policy incentives in making integrated waste-to-fuel systems more attractive to investors.

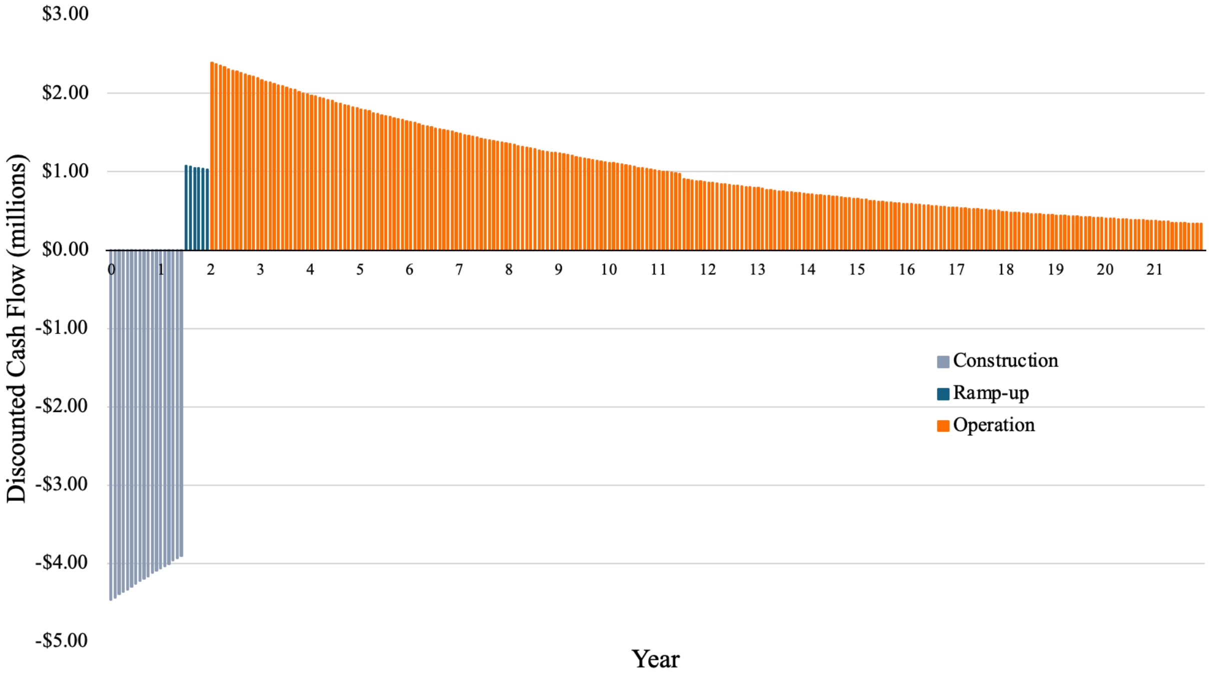

Figure 4.7-1 Individual Discounted Cash Flow Diagram For Scenario 1

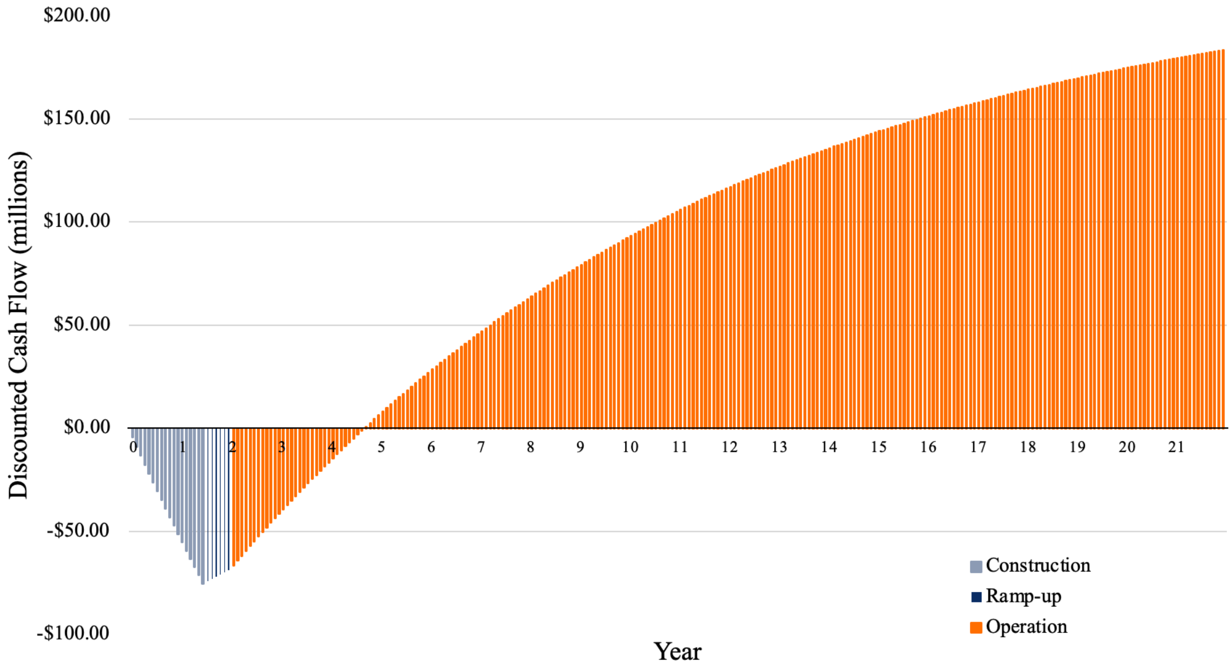

Figure 4.7-2 Cumulative Discounted Cash Flow Diagram for Scenario 1

Compared to the base case, Scenario 1 demonstrates a modest yet meaningful financial improvement, with the ROI increasing to 744% and the IRR rising from 35.76% to 36.29%. This uplift, while numerically small, underscores the compounding value of policy support, specifically, how even a hypothetical $0.70/kg renewable fuel tax credit can enhance long-term cash flow and marginally improve the project's capital efficiency. In capital-intensive systems with long payback periods, these policy levers can play a decisive role in de-risking investments and nudging projects toward stronger financial viability.

4.7.2 Scenario 2: Production of Whey Protein Only

Although the main purpose of this project is to advance sustainability by producing biobutanol as a renewable energy source, nearly all of the projected profit currently comes from the sale of whey protein powder, a valuable co-product. This raises an important question about the economic justification for the more complex and resource-intensive downstream operations required for biofuel production. To evaluate the financial trade offs, we are modeling an alternative scenario in which the plant functions solely as a whey protein facility, removing the biobutanol pathway entirely. By comparing this baseline against the full integrated process using a discounted cash flow (DCF) analysis, we can analyze whether the added costs of pursuing biobutanol are offset by long-term environmental and economic value, or if the more immediate profitability lies in focusing on protein recovery alone. As seen in *Figure 4.7-4*, the DCF breaks even in year 2, as opposed to after 4.5 years in our current project scenario. Producing only whey protein and cutting out the rest of the production process does slightly increase the cumulative DCF, visible in *Figure 4.7-5*.

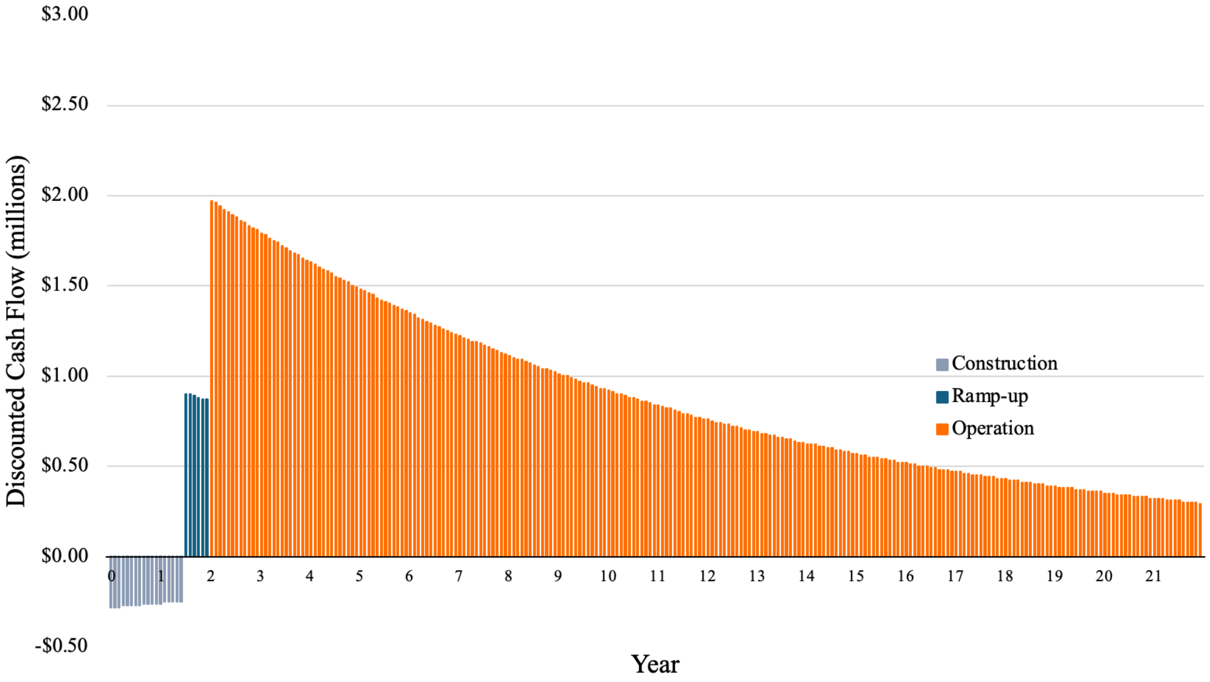

Figure 4.7-3 Individual Discounted Cash Flow Diagram for Scenario 2

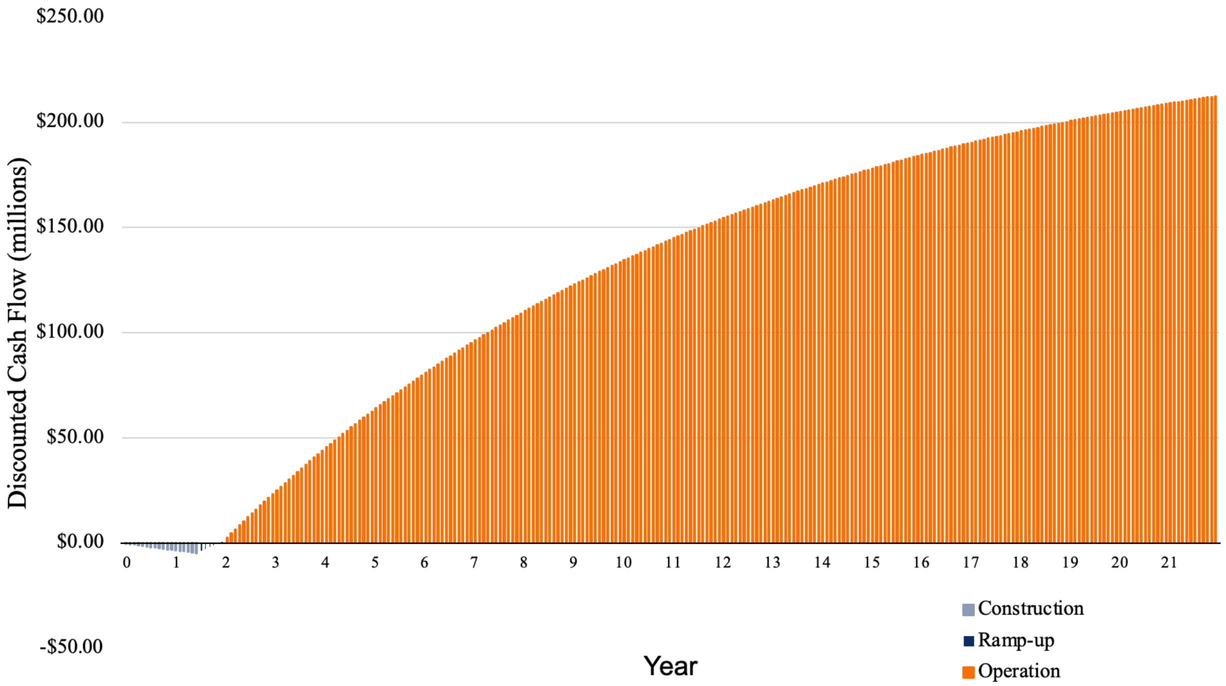

Figure 4.7-4 Cumulative Discounted Cash Flow Diagram for Scenario 2

In Scenario 2, where only whey protein is produced, the financial metrics are significantly stronger, with an ROI of 12,170% and an IRR of 287%. This reflects the extremely high-margin nature of the whey protein stream and the substantial reduction in capital and operational complexity when excluding biobutanol production. While this scenario maximizes financial return, it does so at the expense of the environmental and social co-benefits associated with valorizing the entire waste stream and displacing fossil fuels with renewable butanol. A comparative analysis of the three presented economic scenarios based on their DCF can be in *Figure 4.7-5*.

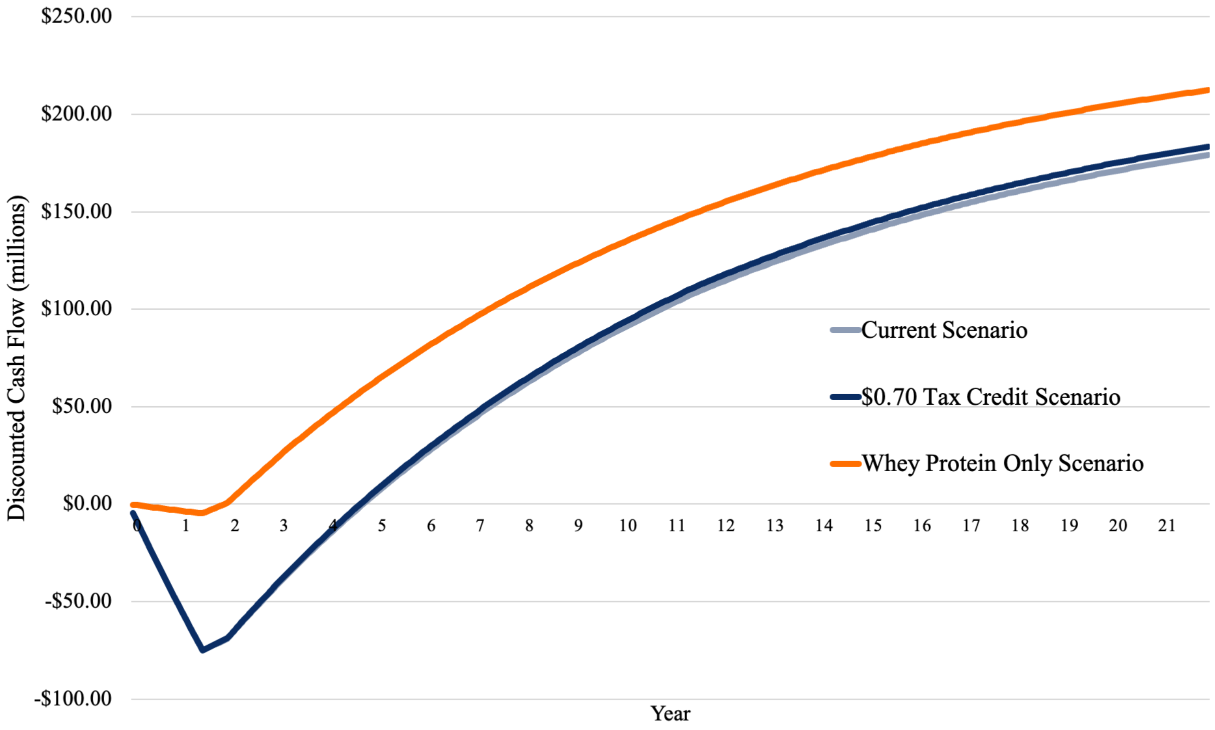

Figure 4.7-5 Comparative Analysis Diagram of Scenarios

When comparing scenarios 1 and 2 to the current status of this project, it is clear that scenario 2, focused solely on producing whey protein powder, yields a higher profit margin. This highlights the substantial capital and operational costs associated with fermentation and separations. While the support of a government implemented policy and tax credits improve returns compared to the current state, the impact is not significant enough to compete with the profitability of exclusive protein powder production. In order for the production of biofuels to become competitive the price of butanol would have to increase, a greater tax credit would have to be implemented, or more cost effective technologies would have to be discovered.

V. ENVIRONMENTAL, SOCIAL, AND SAFETY CONSIDERATIONS

5.1. Environmental Considerations

Though this process is designed to create a cleaner alternative to fossil fuels, it still will have some negative impacts on the environment. Standard operation of the plant will vent approximately 855,000 kilograms of carbon dioxide into the atmosphere per year, furthering greenhouse gas warming and climate change as a whole. Carbon dioxide dissolves in and acidifies water, and is exceedingly difficult to remove from air. These venting operations will also release a stream of approximately 7,920 kg of acetone per year. Acetone is classified as a volatile organic compound (VOC) and contributes to ozone formation in the atmosphere while lowering air quality. Though release amounts and concentrations are fairly low, inhalation of acetone can lead to detrimental health effects. The plant also will require exceedingly large amounts of water and energy. It is estimated that 5.5 billion kilograms of water will be needed for heating and cooling within the plant, which will burden the municipality's water treatment plant and local reservoirs. This water has the ability to be recirculated in the plant up to 50 times, which would lower total water usage and utility costs. About 9.6 million kW-hr of energy will be required to run the plant each year, so this is an expensive project to maintain over a long-term basis.

A positive environmental effect of biobutanol production is the repurposing of a whey waste stream into a set of valuable products. When dumped, acid whey can cause nutrient over-enrichment (eutrophication), damage aquatic ecosystems, and contaminate soil, hindering crop growth. Due to the high organic load of acid whey, energy-intensive secondary waste treatment is likely needed to dispose of such a liquid. Our plant simplifies this challenge by processing the acid whey, resulting in a waste stream composed mostly of water with trace amounts of butanol, ethanol, acetic acid, butyric acid, and *Clostridium* cultures. This effluent is clean enough to require only tertiary wastewater treatment, keeping disposal costs low despite the high volume.

Similarly, vapor emissions from the facility are minimal, as none of the chemicals released fall under the EPA's Hazardous Air Pollutants list and emission levels are low enough that they will not incur fines or cause lasting environmental damage (US EPA, 2016). Carbon dioxide reporting is also not required because the plant operates under the threshold of 25,000 tons of carbon dioxide released per year (Idaho Department of Environmental Quality, 2022). The overall proposed production of biobutanol is advantageous both in its recycling of a waste stream and its creation of a valuable renewable form of energy.

5.2 Social Considerations

The operations of this project are estimated to create over 135 jobs. These roles include operating personnel and site maintenance, providing steady careers for the local community and promoting economic growth. The production of butanol supplies renewable energy to the local economy, creating a circular economy that is environmentally friendly and addresses a traditional waste stream. Increasing local outreach for renewable energy sources has the ability to further support for clean energy within the community and create momentum to replace fossil fuels in the near future. The production and use of biobutanol can also be claimed as a sustainability credit, acting as a benefit to local companies. The plant will be taking up space that could otherwise be used as farm land or housing within the town, which may lead to small-scale conflict. Construction and operation of the plant might cause slight changes in routine for residents, with increased noise pollution and traffic in the town.

5.3 Safety Considerations

Safety is a major priority in the construction of our plant, and worker health must be prioritized to uphold healthy working conditions. By analyzing the hazards associated with each chemical produced in our process, creating a reactivity matrix to identify chemical incompatibilities, and critically thinking about potential spills and how they affect the wellbeing of workers, we can minimize the potential for harm in our plant.

5.3.1 Chemical Hazards & Plant Safety Precautions

The primary chemical hazards for this process are present in components of the downstream separation units. Upstream components are either benign microorganisms in dilute lactose solution or whey protein streams both of which do not present pertinent safety hazards. Components in the downstream process are as follows: water, acetone, butanol, ethanol, acetic acid, butyric acid, and carbon dioxide. Water and carbon dioxide are chemicals that do not present any significant safety hazards in the amounts released, but the other five chemicals exhibit both flammability and minor toxicity hazards.

The major hazards in the downstream process are associated with liquid acetone and butanol. According to Sigma Aldrich Safety Data Sheets, acetone is a category 2 flammable liquid, category 2a eye irritation, and category 3 organ toxicity. Butanol is a category 3 flammable liquid, category 4 oral toxicity, category 2 skin toxicity, category 1 eye toxicity, and category 3 organ toxicity. Ethanol is a category 2 flammable liquid and category 2a eye irritant. Acetic acid is a category 3 flammable liquid, category 1a skin corrosive, and category 1 eye damage. Butyric acid is a category 4 flammable liquid, category 4 oral toxicant, and category 1b skin irritant. All of these chemicals are susceptible to ignition if not stored and handled properly. Other chemical hazards can be found in their corresponding SDS sheets.

To manage waste treatment, all waste streams will be combined and treated using tertiary waste disposal methods. This entails the use of filtration, activated sludge, and chemical processing to turn our waste into environmentally friendly streams. Total waste products are tabulated in *Table 4.4-5*, but consist principally of 189,000,000 kg of water per year and 677,000 kg of *Clostridium acetobutylicum*.

There are working hazards to employees in our plant and safety measures will be taken to protect them. Potential for burns with heated equipment including heat exchangers, fermenters, spray dryer, and distillation columns are present. Heat resistant gloves and flame-retardant lab coats will be used to mitigate this hazard when in contact with materials in these vessels. Spills, electrical wiring, and other slip and fall hazards will be present in the plant, so workers will be trained to be alert and report hazardous floor conditions. Separators, heat exchangers, and pumps have loud, high-power motors, so hearing protection will be used when necessary.

5.3.2 Reactivity Matrix

The reactivity matrix generated in *Figure 5.3-1* shows which chemicals create hazardous conditions when mixed. Caution should be taken when mixing butanol with acetone, butyric acid, and acetic acid, as unstable, explosive, and flammable conditions can be created when heated. Carbon dioxide is corrosive in mixtures with water and acetic acid. Ethanol is flammable and can create explosive reactions with butyric acid or acetic acid. Acetone and ethanol can also be explosive and unstable when heated. None of the chemicals in the reactivity matrix are incompatible, and under normal operating conditions there should not be scenarios where chemicals cause any of the aforementioned hazards.

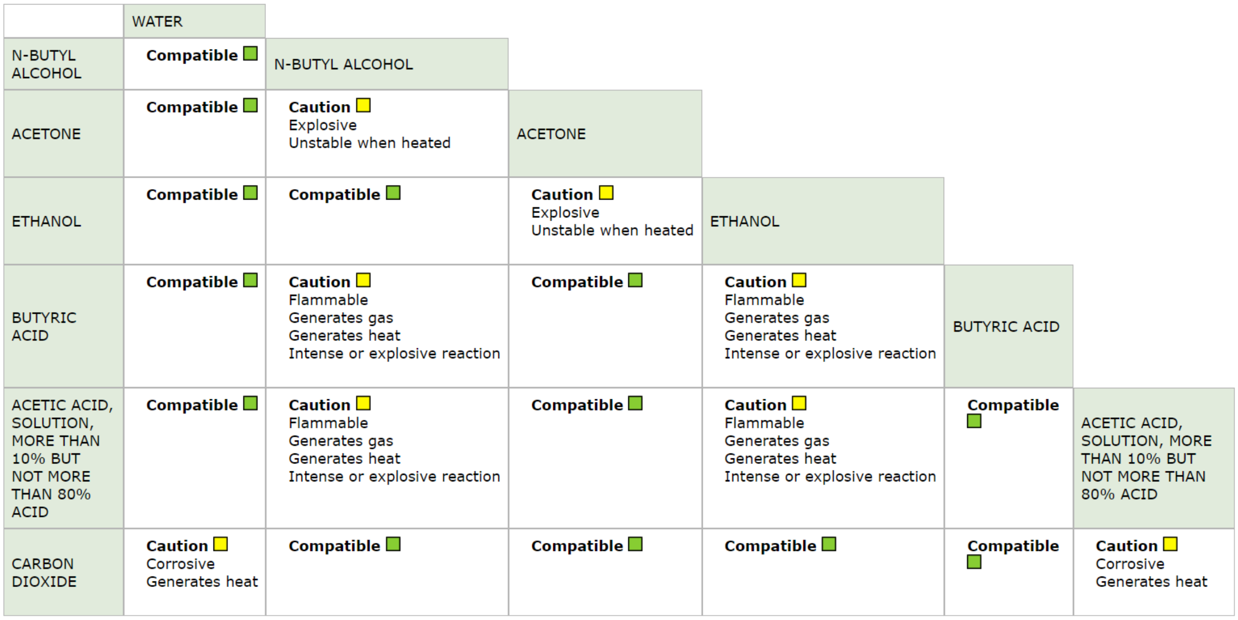

	WATER	N-BUTYL ALCOHOL	ACETONE	ETHANOL	BUTYRIC ACID	ACETIC ACID, SOLUTION, MORE THAN 10% BUT NOT MORE THAN 80% ACID
N-BUTYL ALCOHOL	**Compatible** 🟩					
ACETONE	**Compatible** 🟩	**Caution** 🟨 Explosive Unstable when heated				
ETHANOL	**Compatible** 🟩	**Compatible** 🟩	**Caution** 🟨 Explosive Unstable when heated			
BUTYRIC ACID	**Compatible** 🟩	**Caution** 🟨 Flammable Generates gas Generates heat Intense or explosive reaction	**Compatible** 🟩	**Caution** 🟨 Flammable Generates gas Generates heat Intense or explosive reaction		
ACETIC ACID, SOLUTION, MORE THAN 10% BUT NOT MORE THAN 80% ACID	**Compatible** 🟩	**Caution** 🟨 Flammable Generates gas Generates heat Intense or explosive reaction	**Compatible** 🟩	**Caution** 🟨 Flammable Generates gas Generates heat Intense or explosive reaction	**Compatible** 🟩	
CARBON DIOXIDE	**Caution** 🟨 Corrosive Generates heat	**Compatible** 🟩	**Compatible** 🟩	**Compatible** 🟩	**Compatible** 🟩	**Caution** 🟨 Corrosive Generates heat

Figure 5.3-1 Chemical Reactivity Matrix

5.3.3 Potential Spills and Maximum Credible Event

Three potential spills resulting from gasket ruptures in the distillation column were identified as having the ability to cause environmental and personal safety damage, all of which assume complete releases into the atmosphere and can be found in *Table 5.3-1*. A release in the initial water column would let out 225 kg/hr of butanol and would cause flammability hazards in a 12 yard radius as well as toxicity hazards 23 yards away from the plant, using IDLH standards. IDLH, the metric used to measure the severity of toxic releases, is defined as the concentration of a chemical that poses an immediate risk to life or health. Butanol is not considered an explosive threat, so toxicity hazards pose the largest risk to plant workers. A butanol leak from the volatiles column would cause IDLH toxicity levels 18 yards from the release, and a butanol leak from the final butanol column would also result in IDLH toxicity 18 yards from the plant. The release simulation tool ALOHA was used to source these results given atmospheric conditions in Twin Falls, Idaho (Appendix B). Based on the low potential for large-scale releases from this plant, it is important to educate workers on the risks of butanol spills, but surrounding neighborhoods should not be at risk of hazardous conditions.

Table 5.3-1 Release Scenario Summaries

Source	Chemical (phase)	Hazard	Leak (kg/hr)	Toxicity (IDLH)	Flam. (60% LEL)	Governs
A Water Column	Butanol (l)	Gasket fail	225	23 yds	12 yds	Toxicity
B Volatiles Column	Butanol (l)	Gasket fail	140	18 yds	12 yds	Toxicity
C Butanol column	Butanol (l)	Gasket fail	139	18 yds	12 yds	Toxicity

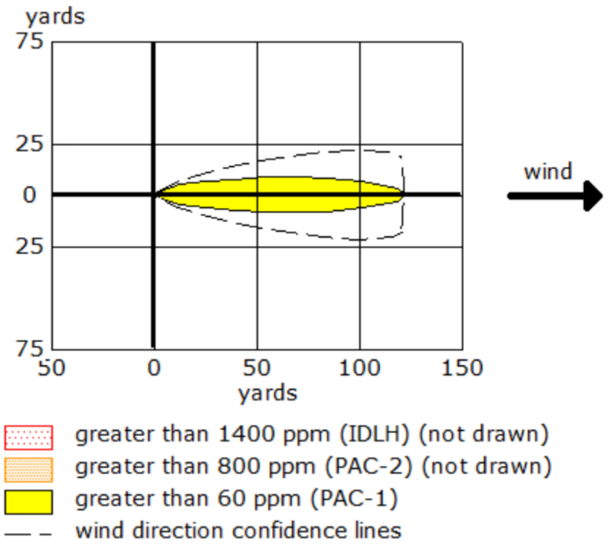

Figure 5.3-2 ALOHA Simulated Release of Butanol in Water Column

VI. FINAL RECOMMENDED DESIGN

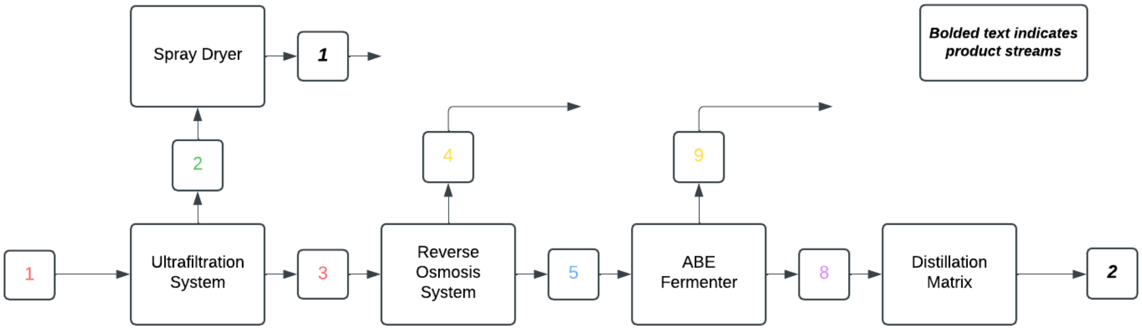

Figure 6.1-1 Full Block Flow Diagram

6.1 Ultrafiltration System

Ultrafiltration uses a small pressure difference to separate particles from liquids through a semipermeable membrane. The system is a tangential filtration system designed to concentrate the protein in the acid whey feed from 2.71 g/L to 16.1 g/L before it enters the spray dryer (H-201). The concentration of protein in the permeate stream entering the reverse osmosis system (R-101 & R-102) is negligible. The feed will be pressurized to 1.6 bar and leave the ultrafiltration system at atmospheric pressure. A summary of the equipment in this block is provided in *Table 6.1-1*, and equipment is shown in *Figure 6.1-2*.

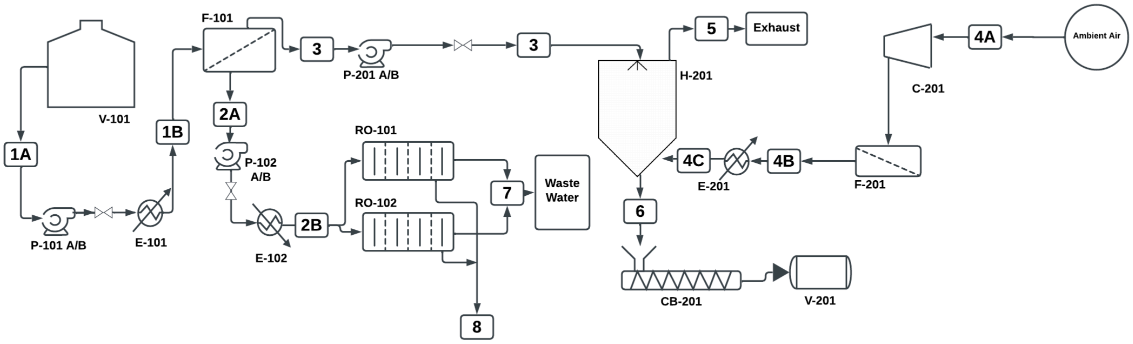

Figure 6.1-2 Upstream Process Flow Diagram

Table 6.1-1 Equipment Summary for Ultrafiltration System

Equipment ID	Equipment Type	Description	Relevant Streams	Specifications
P-101	Acid Whey Feedstock Pump	Takes in acid whey from yogurt plant storage vat	1A	Differential Pressure: 1.95 bar Hydraulic Power: 1.49 kW Electric Draw: 2.21 kW
E-101	Acid Whey Preheater	Heats acid whey to required inlet temperature of 48ºC	1A, 1B	Acid Whey Inlet Temp: 25 ºC Acid Whey Outlet Temp: 48 ºC Steam Pressure: 1 bar Heat Duty: 735 kW Heat Exchanger Area: 312 m^2
F-104	Ultrafiltration System	Concentrates protein content in whey prior to spray drying	1B, 2A, 3	Pressure Drop: >0.52 bar Inlet Pressure: 1.6 bar Outlet Pressure: 1 bar Membrane Area: 34.2 m^2 Operating Temperature: 48 °C

6.2 Spray Dryer

The spray dryer in this design is a counter-current spray dryer. Wet whey protein is flowed into the top of the chamber through a rotary atomizer, which creates droplets. As these droplets fall, they encounter atmospheric air that is heated to 180ºC and then pumped into the bottom of the chamber. As the air rises, it dries the droplets to a maximum moisture level of 3.5%. The dry protein powder is removed from the collection site at the bottom of the dryer. A summary of the equipment in this block is provided in *Table 6.2-1*.

Table 6.2-1 Equipment Summary for Spray Dryer

Equipment ID	Equipment Type	Description	Relevant Streams	Specifications
C-201 A/B	Air Stream Compressor	Brings atmospheric air through the filter and into the spray drying apparatus	4A	Pressure Differential: 1 bar Electric Draw: 904 kW Temperature Differential: 86 ºC
F-201	Air Filter	Takes in atmospheric air and filters it for use in food grade system	4A, 4B,	–
E-201	Air Stream Heater	Heats atmospheric air to required inlet temperature of 180ºC	4B, 4C	Air Inlet Temp: 25 ºC Air Outlet Temp: 180 ºC Steam Pressure: 10 bar Heat Duty: 1471 kW Heat Exchanger Area: 459 m^2
H-201	Spray Dryer	Dries wet whey protein powder to maximum moisture content of 3.5%	3, 4C, 5, 6	Inlet Air Temperature: 180ºC Outlet Air Temperature: 80°C Inlet Whey Temperature: 25ºC Outlet Whey Temperature: 45°C Chamber Height: 7.25m Chamber Diameter: 6.91 m **Rotary Atomizer Specs:** Wheel diameter: 22.0 cm Wheel speed: 15,000 rpm Number of vanes: 20 Vane height: 2.0 cm
P-201 A/B	Wet Whey Pump	Pumps wet whey stream from ultrafiltration into the spray dryer	3	Differential Pressure: 0 bar Hydraulic Power: 0.17 kW Electric Draw: 0.27 kW

6.3 Reverse Osmosis System

Reverse osmosis is a high-pressure filtration process that uses a semi-permeable membrane to separate finer particles, salts, and contaminants from water and is capable of filtering out particles smaller than those removed by ultrafiltration. This particular system is designed to concentrate the lactose content from 39.8 g/L to 99.5 g/L before sending it to our

ABE fermentation storage vat (V-301). The concentration of lactose in the waste stream is negligible. The feed will be pressurized to 60 bar and leave the system at atmospheric pressure. A summary of the equipment in this block is provided in *Table 6.3-1*.

Table 6.3-1 Equipment Summary for Reverse Osmosis System

Equipment ID	Equipment Type	Description	Relevant Streams	Specifications
P-102 A/B	Permeate Pumps	Flows filtered whey permeate into RO system	2A	Differential Pressure: 60.4 bar Hydraulic Power: 42.52 kW Electric Draw: 62.7 kW
E-102	Permeate Cooler	Cools filtered whey permeate to required inlet temperature of 25ºC	2A, 2B	Permeate Inlet Temp: 48 ºC Permeate Outlet Temp: 25 ºC EG Inlet Temp: 5 ºC EG Outlet Temp: 15 ºC Heat Duty: -333 kW Heat Exchanger Area: 45.1 m^2
R-101 & R-102	Reverse Osmosis System	Concentrates lactose content in whey permeate prior to fermentation	2B, 7, 8	Pressure Drop: >58 bar Inlet Pressure: 60 bar Outlet Pressure: ~1 bar Membrane Area: 36 m^2 Operating Temperature: 25°C

6.4 ABE Fermentation Reactors

The proposed ABE fermentation system consists of an upstream 800,000 L storage tank for pre-treatment, followed by ten batch fermentation reactors, each with a working volume of 50,000 L. The fermentation system is designed to convert lactose into acetone, butanol, and ethanol using *Clostridium acetobutylicum*, following Andrews substrate inhibition kinetics (*Equation 3.5-1*).

The reactor dimensions are 3.61 m in diameter and 5.49 m in height, with an impeller size of 1.2 m. The process operates in batch mode to optimize the microbial conversion of lactose to desired products. The operating conditions for the storage tank are maintained between 20°C - 25°C at atmospheric pressure, ensuring proper storage and handling of the pre-treated substrate. The fermentation reactors operate within a temperature range of 33°C - 35°C at atmospheric pressure, optimizing microbial activity for ABE production. The final concentrations post-fermentation are summarized in *Table 6.4-1*. The stream tables for the fermentation segment of the design are shown in Appendix B. Stream 12 shows the total sum of the contents leaving the fermentation reactors. Specific equipment layouts and labels are found in *Figure 6.4-1*.

Table 6.4-1 Fermentation Product Concentrations

Component	Final Concentration
Lactose	0 g/L
Biomass	8.93 g/L
Acetone	5.87 g/L
Butanol	15.0 g/L
Ethanol	1.54 g/L

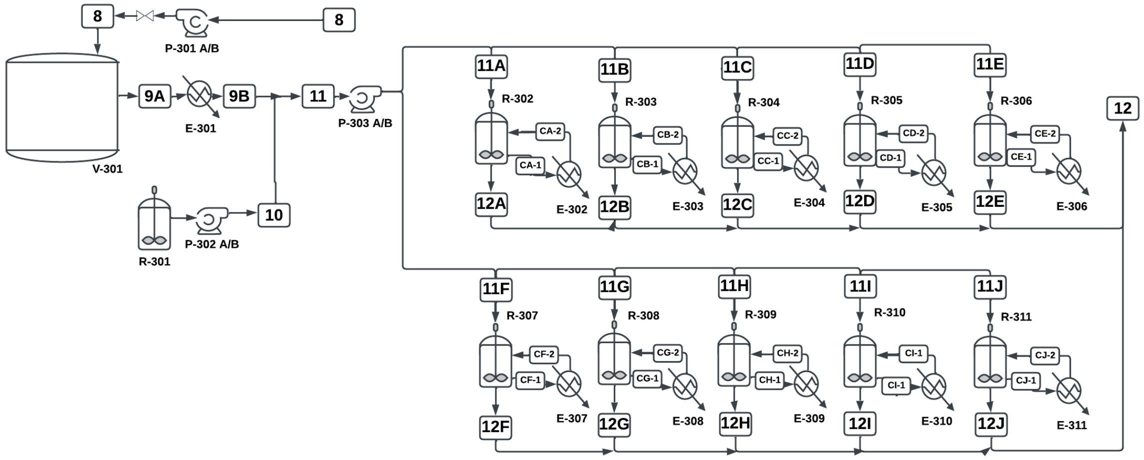

Figure 6.4-1 Fermentation Process Flow Diagram

Table 6.4-2 Equipment Summary for Fermentation

Equipment ID	Equipment Type	Description	Relevant Streams	Specifications
P-301 A/B	Storage Pumps	Pumps lactose rich permeate to fermentation storage tank from RO	8	Differential Pressure: 0 bar Hydraulic Power: 0.56 kW Electric Draw: 0.89 kW
V-301	Storage Tank	Stores concentrated permeate before fermentation	8, 9A	Volume: 800,000 L Temperature: 20°C Pressure: 1 atm
E-301	Substrate Heater	Heats the substrate before it enters the fermentation tanks	9A, 9B	Substrate Inlet Temp: 25 ºC Substrate Outlet Temp: 35 ºC Steam Pressure: 1 bar Heat Duty: 120.6 kW Heat Exchanger Area: 50.2 m^2
R-302 - R-311	Fermentation Tanks	Holds fermentation broth throughout ABE fermentation, uses Rushton impeller to mix	11, 11A - 11J, 12A - 12J, CA-1 - CJ-1, CA-2 - CJ-2, 12	Volume: 50,000 L Temperature: 35°C Pressure: 1 atm Tank Height: 5.49 m Tank Diameter: 3.61 m Impeller Diameter: 1.2 m Jacket Heat Duty: 93 kW
E-302 - E-311	Fermentation Tank Coolers	Provides supplemental cooling to jacketed fermentation tanks to maintain proper temperature	CA-1 - CJ-1, CA-2 - CJ-2	Temperature: 55ºC Cooling Water Inlet Temp: 25ºC Cooling Water Outlet Temp: 34ºC Pressure: 1 bar Heat Duty: 641 kW Heat Exchanger Area: 576 m^2
R-301	Seed Train	Grows *C. acetobutylicum* before use in fermentation	10	Volumes: 50 mL, 1.5 L, 50 L Temperature: 35°C Pressure: 1 atm
P-302 A/B	Seed Train Pumps	Flows the grown cultures into the fermenters	10	Differential Pressure: 0.68 bar Hydraulic Power: 0.00017 kW Electric Draw: 0.00 kW

6.5 Separation System Specifications

In this process, a flash unit, depth filtration system, decanter unit, and five different columns are used to recover acetone, butanol, and ethanol from the fermentation broth. Depth filtration utilizes a porous filter to trap solid particles from a liquid, specifically cell and cell debris downstream from a fermentation system. The system is less prone to clog and can handle a larger volume of particles compared to ultrafiltration. This particular system is designed for complete removal of the cell and cell debris downstream from the fermentation system before the stream is sent to the separation units. The feed will be pressurized to 1.6 bar and leave the system at 1 bar. The depth filter requires backwashing to be performed every 48 hours for 30 minutes, where the backup depth filter will be swapped in as to avoid a lapse in production time. A summary of the equipment in this block is provided in *Table 6.5-2*.

Table 6.5-1 Equipment Summary for F-401 Depth Filtration System

Equipment ID	Equipment Type	Description	Relevant Streams	Specifications
P-401 A/B	Fermentation Product pumps	Flows fermented substrate into the depth filtration unit	13	Differential Pressure: 0.68 bar Hydraulic Power: 0.17 kW Electric Draw: 0.25 kW
F-401	Depth Filtration System	Performs complete removal of cell/cell debris prior to separations	13, 14, 15, 16	Number of Units: 2 Pressure Drop: >0.53 bar Inlet Pressure: 1.6 bar Outlet Pressure: 1 bar System Height: 1.524 m System Diameter: 0.914 m Operating Temperature: 35°C
P-403 A/B	Depth Filtration Backwash Pumps	Pumps water to backwash the depth filtration pumps when scheduled	15	Differential Pressure: 1.28 bar Hydraulic Power: 0.004 kW Electric Draw: 0.01 kW

The isolated fermentation product stream-14 serves as a feed stream to the T-401, Water Column 1. This column aims to remove most of the water, acetic acid, butyric acid, and trace carbon dioxide from the feed. The column operates at 1.5 bar, has a total of 22 stages with a feed on stage 12, and a reflux ratio of 10. A partial vapor-liquid condenser is utilized which operates at 35 ºC and a pressure of 1 bar is set across the column. The bottom product stream-19 has a flow rate of 7,757 kg/hr, with a 0.99 mass fraction of water. The column has a 90%, 88%, and 99% extraction rate of water, butyric acid, and acetic acid respectively. 70% of CO_2 is vented via the top vapor stream-17 and 0% of ABE products were lost to the bottoms stream-18. Stream-18, the resulting liquid distillate stream, is fed into the Volatiles Column (T-402).

Table 6.5-2 Equipment Summary for T-401 Water Column 1

Equipment ID	Equipment Type	Description	Relevant Streams	Specifications
T-401	Water Column 1	Distillation Column that aims to remove water, acids, and carbon dioxide	14, 17, 18, 19	Number of Stages: 22 Feed Stage: 12 Diameter: 2 m Total Height: 16.5 m Operating Pressure: 1 bar Condenser Temperature: 35 ºC Reflux Ratio: 10
P-403 A/B	Post-Depth Filtration Pumps	Pumps the filtered medium into the first separations unit T-401	14	Differential Pressure: 1.68 bar Hydraulic Power: 0.42 kW Electric Draw: 0.40 kW
P-404 A/B	Water Column 1 Reflux Pumps	Flows distillate reflux back into T-401 and also feeds liquid distillate to T-402	18	Differential Pressure: 1.35 bar Hydraulic Power: 0.087 kW Electric Draw: 0.13 kW
P-405 A/B	Water Column 1 Bottoms Pump	Flows liquid bottoms to waste water treatment	19	Differential Pressure: 1.85 bar Hydraulic Power: 0.05 kW Electric Draw: 0.19 kW
E-401	Water Column 1 Overhead Condenser	Condenses T-401 distillate using cooling water	C1A, C1B	Distillate Inlet Temp: 110 ºC Distillate Outlet Temp: 35 ºC CW Inlet Temp: 25 ºC CW Outlet Temp: 35 ºC Heat Duty: -7,347 kW Heat Exchanger Area: 218 m^2
E-402	Water Column 1 Reboiler	Heats Column T-401	R1A, R1B	Bottoms inlet Temp: 112 ºC Bottoms Outlet Temp: 112 ºC Steam Inlet Temp: 170 ºC Steam Outlet Temp: 112 ºC Heat Duty: 8,036 kW Heat Exchanger Area: 140 m^2

The Volatiles column, T-402, aims to strip acetone and ethanol into the distillate stream-21 and Water and Butanol in the bottoms stream-22. The column operates at 1 bar, has a total of 29 stages with a feed on stage 15, and a reflux ratio of 20. T-402 operates with a partial vapor-liquid condenser operating at 35 ºC and 1 bar to allow any residual carbon dioxide to be released as a vapor stream while maintaining a high purity liquid distillate stream. The distillate product stream-21 has a total flow rate of 80 kg/hr, 96% of the inlet acetone and 87% of the inlet ethanol are retained in the distillate stream-21, while the bottoms stream-21 has a flow rate of 995 kg/hr and retains 99% of the inlet butanol and water. The tops stream-21 is sent to the Acetone Ethanol Column (T-403) while the bottoms stream-22 is sent to the Water Column 2 (T–404) and the TCD.

Table 6.5-3 Equipment Summary for T-402 Volatiles Column

Equipment ID	Equipment Type	Description	Relevant Streams	Specifications
T-402	Volatiles Column	Distillation Column that separates the volatile components from the heavier ones	18, 20, 21, 22	Number of Stages: 29 Feed Stage: 15 Diameter: 1 m Total Height: 21 m Operating Pressure: 1 bar Condenser Temperature: 35 ºC Reflux Ratio: 20
P-406 A/B	Volatiles Column Reflux Pumps	Flows distillate reflux back into T-402 and feeds liquid distillate to T-403	21	Differential Pressure: 1.35 bar Hydraulic Power: 0.0057 kW Electric Draw: 0.01 kW
P-407 A/B	Volatiles Column Bottoms Pumps	Flows heavier components to T-404	22	Differential Pressure: 3.13 bar Hydraulic Power: 0.74 kW Electric Draw: 0.09 kW
E-403	Volatiles Column Overhead Condenser	Condenses T-402 distillate using cooling water	C2A, C2B	Distillate Inlet Temp: 71 ºC Distillate Outlet Temp: 35 ºC CW Inlet Temp: 25 ºC CW Outlet Temp: 35 ºC Heat Duty: -428 kW Heat Exchanger Area: 31 m^2
E-402	Volatiles Column Reboiler	Heats Column T-402	R2A, R2B	Bottoms inlet Temp: 91 ºC Bottoms Outlet Temp: 91 ºC Heat Duty: 493 kW Heat Exchanger Area: 77 m^2

The Acetone Ethanol column (T-403) separates acetone and ethanol in the tops and bottoms products respectively. It operates at 1 bar, has a total of 22 stages, feeds to stage 12 and has a reflux ratio of 20. T-403 with a full condenser operating at 35 ºC and 1 bar. The overhead distillate stream-23 contains the final acetone product, which has a flow rate of 54 kg/hr with a 99.9 w% purity. Due to the small quantity of ethanol produced in ABE fermentation, it is not recovered in a pure enough stream to be sold as a product. Therefore, the bottoms steam-23 is being considered as waste, a possible use of which is to flare this stream and use it as a fuel source, potentially reducing waste disposal and energy costs.

Table 6.5-4 Equipment Summary for T-403 Acetone Ethanol Column

Equipment ID	Equipment Type	Description	Relevant Streams	Specifications
T-403	Acetone Ethanol Column	Distillation Column that isolates Acetone and Ethanol	21, 23, 24	Number of Stages: 22 Feed Stage: 12 Diameter: 0.5 m Total Height: 16.5 m Operating Pressure: 1 bar Condenser Temperature: 35 ºC Reflux Ratio: 20
P-408 A/B	Acetone Ethanol Column Reflux Pumps	Flows reflux distillate back into T-403 and liquid distillate stream to product	23	Differential Pressure: 1.35 bar Hydraulic Power: 0.0017 kW Electric Draw: 0.00 kW
P-409 A/B	Acetone Ethanol Bottoms Pumps	Flows bottoms to waste water treatment	24	Differential Pressure: 1.85 bar Hydraulic Power: 0.008 kW Electric Draw: 0.00 kW
E-405	Acetone Ethanol Overhead Condenser	Condenses T-403 vapor distillate using cooling water	C3A, C3B	Distillate Inlet Temp: 56 ºC Distillate Outlet Temp: 35 ºC CW Inlet Temp: 25 ºC CW Outlet Temp: 35 ºC Heat Duty: -178 kW Heat Exchanger Area: 17 m^2
E-406	Acetone Ethanol Reboiler	Heats the Acetone Ethanol Column	R3A, R3B	Bottoms inlet Temp: 81 ºC Bottoms Outlet Temp: 81 ºC Heat Duty: 179 kW Heat Exchanger Area: 2.7 m^2

T-404 the Water Column 2 separates a butanol-water azeotrope stream-25 in the distillate and a water stream in the bottoms stream-30. It operates at 1 bar, has a total of 15 stages, and feeds both the initial feed stream-22 and an aqueous recycle stream-28 on tray 15 replacing a reflux stream. The bottoms stream has a flow rate of 846 kg/hr, is 99 w% water, and contains 0% butanol. This stream is sent to a wastewater treatment plant. The distillate stream-25 contains all of the fed butanol with a total flow rate of 613 kg/hr. This distillate is then mixed with the other butanol-water stream-26 from T-405 which is condensed and sent to decanter D-401 to be separated.

Table 6.5-5 Equipment Summary for T-404 Water Column 2

Equipment ID	Equipment Type	Description	Relevant Streams	Specifications
T-404	Water Column 2	Distillation Column that separates water from butanol-water azeotrope	22, 25, 28, 30	Number of Stages: 15 Feed Stage: 1 Diameter: 0.5 m Total Height: 12.5 m Operating Pressure: 1 bar Condenser Temperature: N/A Reflux Ratio: N/A
P-410 A/B	Decanter Aqueous Phase Pump	Flows aqueous phase from decanter into the top of T-404	28	Differential Pressure: 3.13 bar Hydraulic Power: 0.36 kW Electric Draw: 0.04 kW
P-412 A/B	Water Column 2 Bottoms Pumps	Flows bottoms from T-404 to waste water	30	Differential Pressure: 1.85 bar Hydraulic Power: 0.4 kW Electric Draw: 0.02 kW
E-407	Water Column 2 Reboiler	Heats column T-404	R4A, R4B	Bottoms Inlet Temp: 100 ºC Bottoms Outlet Temp: 100 ºC Steam Inlet Temp: 170 ºC Steam Outlet Temp: 100 ºC Heat Duty: 317 kW Heat Exchanger Area: 4.5 m^2

D-401 the decanter unit separates the butanol-water azeotrope into a aqueous phase stream-28 that is water rich and an organic phase stream-29 that is butanol rich. The aqueous phase stream-22 is sent back into T-404 as a reflux, and the organic phase stream-29 is sent to

T-405 as the initial feed stream. This decanter unit operates at 1 bar and 35 ºC and has dimensions as listed below.

Table 6.5-6 Equipment Summary for Decanter

Equipment ID	Equipment Type	Description	Relevant Streams	Specifications
D-401	Decanter Unit	Separates the butanol rich organic phase from water rich aqueous phase	27, 28, 29	Volume Capacity: 2.4 m^3 Diameter: 1 m Height: 4 m Operating Pressure: 1 bar Operating Temperature: 35 ºC
E-409	Azeotrope Condenser	Condenses Mixed Azeotrope into liquid for feeding into D-401	25, 26, 27	Bottoms Inlet Temp: 95 ºC Bottoms Outlet Temp: 35 ºC CW Inlet Temp: 25 ºC CW Outlet Temp: 35 ºC Heat Duty: -185 kW Heat Exchanger Area: 11 m^2

The end product of butanol is separated out in the bottoms stream-31 of the Butanol Column T-405. This column operates at 1 bar, contains 15 stages, and has a single feed stream on stage 15 replacing a reflux stream and requiring no condenser. The overhead vapor stream-26 is a butanol-water azeotrope which is sent to be mixed with the other butanol-water azeotrope stream-25 from T-404, is condensed in E-409, and separated into organic and aqueous phases in decanter D-401. The bottoms stream-31 contains the final butanol product, it has a total flow rate of 149 kg/hr with a 93.3 wt% purity in terms of butanol. This stream is sent storage vessel V-406. The arrangement of all aforementioned equipment is displayed in *Figure 6.5-1*.

Table 6.5-7 Equipment Summary for Butanol Column

Equipment ID	Equipment Type	Description	Relevant Streams	Specifications
T-405	Butanol Column	Distillation Column that separates butanol product from butanol rich azeotrope	26, 29, 31	Number of Stages: 15 Feed Stage: 1 Diameter: 0.5 m Total Height: 12.5 m Operating Pressure: 1 bar Condenser Temperature: N/A Reflux Ratio: N/A
P-411 A/B	Decanter Organic Phase Pumps	Feeds butanol rich organic phase to column T-405	29	Differential Pressure: 2.54 bar Hydraulic Power: 0.01 kW Electric Draw: 0.01 kW
P-413 A/B	Butanol Column Bottoms Pumps	Flows liquid bottoms to butanol product	31	Differential Pressure: 1.85 bar Hydraulic Power: 0.4 kW Electric Draw: 0.02 kW
E-406	Butanol Column Reboiler	Heats Butanol Column	R5A, R5B	Bottoms inlet Temp: 99 ºC Bottoms Outlet Temp: 99 ºC Heat Duty: 42 kW Heat Exchanger Area: 1 m^2

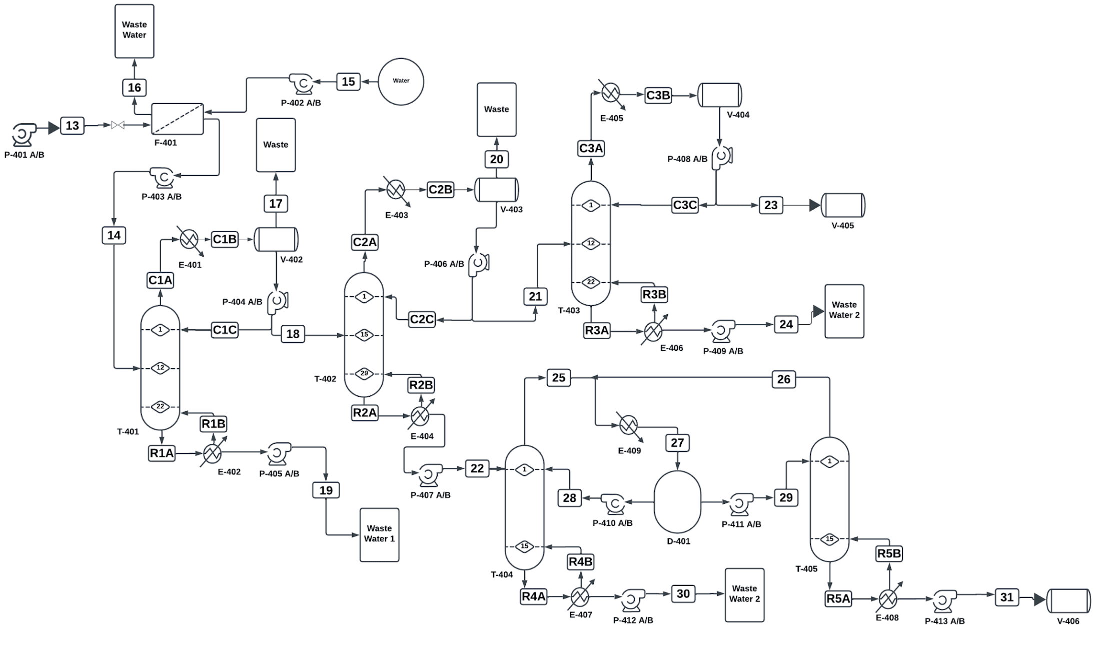

Figure 6.5-1 Separation System Process Flow Diagram

VII. CONCLUSIONS & RECOMMENDATIONS

7.1 Conclusions and Recommendations for Pretreatment

The pretreatment section of the design, consisting of ultrafiltration, spray drying, and reverse osmosis, are common yet essential processes in industry, particularly in food production and waste processing. Drawing on existing research, this report defines unit specifications and dimensions for a unique feedstock: acid whey. Much of the equipment required is expensive and large and consumes a hefty amount of electricity and other utilities, making this a process only large-scale and well-established companies are able to implement. There is potential to optimize filter types, materials, and configurations to reduce fouling and lower both capital and utility costs. Innovations in spray dryer technology, such as nozzle design, airflow dynamics, and the introduction of drying aids and other additives, could enhance spray dryer performance and improve product quality.

7.2 Conclusions and Recommendations for Fermentation

To improve fermentation yields and efficiency, it is recommended to employ a series of improvements compared to the proposed model. A large number of additives can enhance microbial activity, including nitrogen sources such as peptones and yeast and ammonium sulfate. Buffering agents can be used to stabilize pH values during acidogenesis and solventogenesis to lower the concentration of butyric and acetic acid intermediates. Metal ions and salts are often sometimes used to increase enzymatic activity and support cell growth. A combination of these factors along with other additives can help support bacterial growth. Since acid whey waste as a substrate is not heavily studied, changing the microbial strain may also increase yields and lower fermentation time. *Clostridium beijerinckii*, more highly specialized strains of *Clostridium* *acetobutylicum*, and *Clostridium saccharobutylicum* are potential alternatives that can be tested at a lab scale.

ABE fermentation modifications may also help increase butanol concentrations and lower the environmental footprint of the process. Gas stripping is a commonly used method to enhance ABE fermentation which bubbles inert gases through the fermentation reactor to collect solvents. The solvents are then removed from the reactor and sent to separation processes. By keeping butanol concentrations below the 15 g/L toxicity threshold, *C. acetobutylicum* can produce butanol for longer time periods and increase yields. Another addition to the fermentation process that would focus on positive environmental efforts would be utilizing carbon capture. Trapping the carbon dioxide formed by fermentation and sequestering it or using it to create synthetic fuels can help offset environmental impact from this biofuel-producing plant. Though the process created was run using batch fermentation, fed-batch and continuous fermentation are other methods which have shown potential to increase the scale of production and lower waste. Overall, vigorous research and experimentation should be performed before starting up the plant to maximize the positive effects of process parameters and mitigate the weaknesses that lower the plant's profitability.

7.3 Conclusions and Recommendations for Separations

The primary recommendation surrounding the separations block is to further optimize the distillation sequence. Based upon the current Aspen Plus V14 model, the purity of the ethanol product stream is not high enough to be sold. In addition, much of the equipment's capital costs are high and draw a high amount of utilities such as steam. To remedy these concerns, further optimization of column parameters like reflux ratio, number of trays, feed location, and operating pressure could be employed. A method for completing this could be to utilize Aspen Plus V14's built-in optimization feature, taking the manually optimized parameters described in this paper as a base line and allowing the software to conduct the rest.

Another recommendation is to study the impact of recovering acetone and other trace solvents from carbon dioxide vapor streams. By adding in additional condensers to recover some solvents, an offset in cost could be observed. Furthermore, optimizing the partial condensers and initial flash unit to reduce the amount of solvents lost could similarly result in higher performance. Overall further study and optimization of all equipment could lead to greater results in profitability.

7.4 Conclusions and Recommendations for Economic Viability

Based on the comprehensive technical and economic evaluation, the project to convert excess yogurt waste into both whey protein and biobutanol is a clear "go." While the highest profitability occurs when focusing solely on whey protein production (as shown in Scenario 2), the addition of biobutanol production still yields significant profitability and unlocks key non-monetary benefits. The full system captures economic value from what would otherwise be waste, turning an environmental liability into dual revenue streams—protein for the food market and butanol as a renewable fuel.

From a policy standpoint, the potential for renewable fuel tax credits, such as the $0.70/kg incentive modeled in Scenario 1, further strengthens the case. Although we do not currently have direct access to such a credit, if this or a similar incentive were to become available, it would significantly enhance project economics, especially for the butanol stream, and accelerate return on investment. It would also signal stronger institutional support for renewable fuels, making this kind of circular economy project even more attractive. Given these considerations, including the significant positive social and environmental externalities, we recommend moving forward with the full original design.

Beyond economics, this integrated approach aligns with broader sustainability and social goals. It reduces the environmental burden of whey disposal, supports rural economies, and contributes to decarbonization via renewable biofuel production. Therefore, considering the project's financial robustness, the availability of tax incentives, and its positive environmental and social externalities, we recommend proceeding with the full original design that includes both whey protein and biobutanol production. This strategy best capitalizes on both profitability and purpose.

VIII. ACKNOWLEDGEMENTS

We would like to express our gratitude to the University of Virginia Chemical Engineering Department for providing the resources and instruction that made this project possible. Their commitment to fostering a strong foundation in engineering principles and practical design has been instrumental in our progress. Likewise, we are deeply grateful to our technical advisor, Professor Eric Anderson, for his unwavering support, insightful feedback, and encouragement throughout the completion of this project.

IX. REFERENCES

Afshar Ghotli R., Shafeeyan M. S., Abbasi M. A., Raman A. C., Ibrahim S. Macromixing study for various designs of impellers in a stirred vessel // Chemical Engineering and Processing: Process Intensification. 2020. Vol. 148. p. 107794.

Blignault Van Der Merwe, A., Knoetze, J., & Görgens, J. (2010). *Evaluation of Different Process Designs for Biobutanol Production from Sugarcane Molasses*. https://crses.sun.ac.za/old/files/research/completed-research/bio_energy/ab_van_der_merwe.pdf

Chapple, D., Kresta, S. M., Wall, A., & Afacan, A. (2002). The effect of impeller and tank geometry on power number for a pitched blade turbine. *Chemical Engineering Research and Design, 80*(4), 364–372. https://doi.org/10.1205/026387602760213271

Charles, D. (2012). "Why Greek Yogurt Makers Want Whey to Go Away." *NPR.org*, www.npr.org/sections/thesalt/2012/11/21/165478127/why-greek-yogurt-makers-want-whey-to-go-away.

Cheng, W., Gong, L., Chen, C. et al. High butanol/acetone ratio featured ABE production using mixture of glucose and waste Pichia pastoris medium-based butyrate fermentation supernatant. Bioprocess Biosyst Eng 45, 465–480 (2022). https://doi.org/10.1007/s00449-021-02671-y

Culligan International. (2004). *Fundamentals of depth filtration*. Culligan Industrial Water. https://www.culliganindustrialwater.com/wp-content/uploads/fundamentals_of_depth_filtration.pdf

DairyRO. (n.d.). Hydranautics Nitto Group Company. https://membranes.com/solutions/products/process/dairyro/

Darkwah, K., Nokes, S. E., Seay, J. R., & Knutson, B. L. (2018). Mechanistic simulation of batch acetone–butanol–ethanol (ABE) fermentation with in situ gas stripping using Aspen Plus™. *Bioprocess and Biosystems Engineering, 41*(10), 1283–1294. https://doi.org/10.1007/s00449-018-1956-6

Datt, P. (2011). Latent Heat of Vaporization/Condensation. In: Singh, V.P., Singh, P., Haritashya, U.K. (eds) Encyclopedia of Snow, Ice and Glaciers. Encyclopedia of Earth Sciences Series. Springer, Dordrecht. https://doi.org/10.1007/978-90-481-2642-2_327

El-Gazzar, F.E., Marth, E.H. (1991). Ultrafiltration and Reverse Osmosis in Dairy Technology: A Review. *Journal of Food Protection, 54*(10), 801-809. doi: 10.4315/0362-028X-54.10.801

Engineeringtoolbox, E. (2025, March 4). *Ethylene glycol heat-transfer fluid properties: Density, Data & Charts*. Engineering ToolBox. https://www.engineeringtoolbox.com/ethylene-glycol-d_146.html

Engineeringtoolbox, E. (2025b, March 4). *Specific heat capacity of water: Temperature-dependent data and calculator*. Engineering ToolBox. https://www.engineeringtoolbox.com/specific-heat-capacity-water-d_660.html

Engineering ToolBox. (n.d.). *Air density and specific weight*. https://www.engineeringtoolbox.com/air-density-specific-weight-d_600.html

Erickson, B. E. (2017). All the whey. Chemical & Engineering News. https://cen.acs.org/articles/95/i6/Acid-whey-waste-product-untapped.html

Ezeji, T.C., Qureshi, N., Blaschek, H.P., Acetone butanol ethanol (ABE) production from concentrated substrate: reduction in substrate inhibition by fed-batch technique and product inhibition by gas stripping, Appl Microbiol Biotechnology, 2004, DOI 10.1007/s00253-003-1400-x

Ghaly, A. E., Kamal, M., & Correia, L. R. (2005). Kinetic modelling of continuous submerged fermentation of cheese whey for single cell protein production. *Bioresource Technology, 96*(10), 1143–1152. https://doi.org/10.1016/j.biortech.2004.09.002

Hartline, R. (2022, January 13). Microbiology Laboratory Manual (Hartline). Biology LibreTexts. https://bio.libretexts.org/Bookshelves/Microbiology/Microbiology_Laboratory_Manual

Idaho Department of Environmental Quality. (2022). Air quality permitting. Idaho DEQ. https://www.deq.idaho.gov/permits/air-quality-permitting/

Junker, B., Stanik, M., Barna, C. et al. Influence of impeller type on mass transfer in fermentation vessels. Bioprocess Engineering 19, 403–413 (1998). https://doi.org/10.1007/s004490050540

Kennedy, S. (2017). "Inside the Yogurt Plant: Chobani Looms Large in Magic Valley." Dairy Foods. www.dairyfoods.com/articles/92300-inside-the-yogurt-plant-chobani-looms-large-in-magic-valley.

Khamaiseh, E. I., Abdul Hamid, A., Abdeshahian, P., Wan Yusoff, W. M., & Kalil, M. S. (2014). Enhanced butanol production by Clostridium acetobutylicum NCIMB 13357 grown on date fruit as carbon source in P2 medium. *The Scientific World Journal*. https://doi.org/10.1155/2014/395754

Hoppe, K., Wischemann, L., Schaldach, G., Zielke, R., Tillmann, W., Thommes, M., & Pieloth, D. (2023). Filtration kinetics of depth filters—Modeling and comparison with tomographic data of particle depositions. *Atmosphere, 14*(4), 640. https://doi.org/10.3390/atmos14040640

Lin, Z.; Cong, W.; Zhang, J. Biobutanol Production from Acetone–Butanol–Ethanol Fermentation: Developments and Prospects. *Fermentation* 2023, 9, 847. https://doi.org/10.3390/fermentation9090847

Ling, K. (2008). *Whey to Ethanol: A Biofuel Role for Dairy Cooperatives*. USDA Rural Development. https://www.rd.usda.gov/files/RR214.pdf

Liu, G., Si, Z., Chen, B., Chen, C., Cheng, S., Ouyang, J., Chen, H., Cai, D., Qin, P., & Wang, J. (2022). Selection of eco-efficient downstream distillation sequences for acetone-butanol-ethanol (ABE) purification from in situ product recovery system. *Renewable Energy*, *185*, 17–31. https://doi.org/10.1016/j.renene.2021.11.033

López-Contreras, A., Claassen, P., Mooibroek, H. et al. (2000). Utilisation of saccharides in extruded domestic organic waste by Clostridium acetobutylicum ATCC 824 for production of acetone, butanol and ethanol. Appl Microbiol Biotechnol 54, 162–16. https://doi.org/10.1007/s002530000374

McDonald, E. J., & Turcotte, A. L. (1948). *Density and refractive indices of lactose solutions*. Journal of Research of the National Bureau of Standards, 41(1), 63–67. https://nvlpubs.nist.gov/nistpubs/jres/041/jresv41n1p63_A1b.pdf

Md Razali NAA, Ibrahim MF, Kamal Bahrin E, Abd-Aziz S. Optimisation of Simultaneous Saccharification and Fermentation (SSF) for Biobutanol Production Using Pretreated Oil

Palm Empty Fruit Bunch. Molecules. 2018 Aug 3;23(8):1944. doi: 10.3390/molecules23081944.

Mujumdar, A. S., & Jog, V. M. (1977). *Simple procedure for design of a spray dryer*. https://www.researchgate.net/publication/293304987

Safe Drinking Water Foundation. (2025). *Ultrafiltration, nanofiltration and reverse osmosis.* Safe Water. https://www.safewater.org/fact-sheets-1/2017/1/23/ultrafiltrationnanoandro

Paredes, I., Quintero, J., Guerrero, K., Gallardo, R., Mau, S., Conejeros, R., Gentina, J.C., Aroca, G. (2021), Kinetics of ABE fermentation considering the different phenotypes present in a batch culture of Clostridium beijerinckii NCIMB-8052, Electronic Journal of Biotechnology, 2022,, https://doi.org/10.1016/j.ejbt.2021.12.002.

PowderProcess.net. (n.d.). *Spray dryer chamber configuration: Co-current, counter-current, mixed flow*, https://powderprocess.net/Spray_Drying/Spray_Drying_Current.html

Procentese, A., Raganati, F., Olivieri, G., Russo, M. E., Salatino, P., & Marzocchella, A. (2015). Continuous lactose fermentation by Clostridium acetobutylicum--assessment of solventogenic kinetics. Bioresource technology, 180, 330–337. https://doi.org/10.1016/j.biortech.2015.01.008

Syed, Q. (1994). Biochemical Studies on Anaerobic Fermentation of Molasses by Clostridium Acetobutylicum. Lahore: University of the Punjab.

Synder Filtration. (n.d.). *ST (PES 10,000Da) Sanitary UF Membrane.* https://synderfiltration.com/st-pes-10kda-sanitary/

Tax Foundation. (2025, January 21). *State corporate income tax rates and brackets for 2025*. https://taxfoundation.org/data/all/state/state-corporate-income-tax-rates-brackets/

Towler, G. & Sinnott, Ray. (2022). Chemical Engineering Design - Principles, Practice and Economics of Plant and Process Design (3rd Edition). Elsevier https://app.knovel.com/hotlink/pdf/id:kt012WN1S1/chemical-engineering/fixed-capital-investment

Turton, R., Bailie, R. C., Whiting, W. B., Shaeiwitz, J. A., & Bhattacharyya, D. (2012). *Analysis, Synthesis, and Design of Chemical Processes* (4th ed.). Pearson.

US EPA, O. (2015, December 16). Initial List of Hazardous Air Pollutants with Modifications. Www.epa.gov. https://www.epa.gov/haps/initial-list-hazardous-air-pollutants-modifications#mods

Zhang, Q., Wu, D., Lin, Y., Wang, X., Kong, H., and Tanaka, S., Substrate and Product Inhibition on Yeast Performance in Ethanol Fermentation, Energy & Fuels 2015 29 (2), 1019-1027 DOI:10.1021/ef502349v

Zydney, A. L., & van Reis, R. (2011). Bioseparations: Membrane processes. In M. Moo-Young (Ed.), *Comprehensive biotechnology* (2nd ed., pp. 499-520). Academic Press. https://doi.org/10.1016/B978-0-08-088504-9.00440-2

X. APPENDIX

Appendix A: Incoming Whey Flow Rate Calculations

$$\frac{5.3\text{ oz}}{\text{yogurt}} = \frac{\overset{\smile}{3}\text{ cups}}{1\text{ lb yo.}}$$

$$\underbrace{\boxed{\frac{40{,}000\text{ cups}}{\text{hr}}}}_{\text{(Kennedy, 2017)}} \cdot \frac{1\text{ lb yo.}}{3\text{ cups}} \cdot \underbrace{\boxed{\frac{4\text{ lb whey}}{1\text{ lb yo.}}}}_{\text{(Charles, 2017)}} \cong \frac{60{,}000\text{ lb whey}}{\text{hr}} = \boxed{\frac{27{,}200\text{ kg whey}}{\text{hr}}}$$

Appendix B: Stream Tables

Pretreatment Process Stream Table (kg/hr)

	1A	1B	2A	2B	3	4A	4B	4C	5	6	7	8
Whey Protein Solids	969	969	0	0	969	0	0	0	0	969	0	0
Air	0	0	0	0	0	33730	33730	33730	33730	0	0	0
Lactose	993	993	993	993	0	0	0	0	0	0	0	993
H_2O	25253	25253	23969	23969	1284	0	0	0	1249	35	14967	8986
Totals	**27215**	**27215**	**24962**	**24962**	**2253**	**33730**	**33730**	**33730**	**34979**	**1004**	**14967**	**9979**

Fermentation Process Stream Table (kg/hr)

	8	9A	9B	10	11	11 A - 11 J	12 A - 12 J	12	Combined Vent Stream
CO_2	0	0	0	0	0	0	27.02	270.21	260
Acetone, C_3H_6O	0	0	0	0	0	0	5.60	56.04	1
Acetic Acid, $C_2H_4O_2$	0	0	0	0	0	0	0.29	2.88	0
Butanol, $C_4H_{10}O$	0	0	0	0	0	0	14.31	143.13	0
Butyric Acid, $C_4H_8O_2$	0	0	0	0	0	0	0.76	7.65	0
Ethanol, $C_2H_6O_2$	0	0	0	0	0	0	1.48	14.79	0
C. acetobutylicum	0	0	0	9.56	9.56	0.96	8.54	85.42	0
Lactose	993	993	993	0	993	99.30	0	0	0
H_2O	8986	8986	8986	0	8986.0	898.60	845.03	8450.30	2
Totals	9979	9979	9979	9.56	9988.56	998.86	903.04	9030.40	263

Separations Process Stream Table (kg/hr)

	13	14	15	16	17	18	19	20	21	22	23	24	25	26	27	28	29	30	31
CO_2	10	10	0	0	7	3	0	3	1	0	1	0	0	0	0	0	0	0	0
Acetone, C_3H_6O	55	55	0	0	0	55	0	2	53	0	52	1	0	0	0	0	0	0	0
Acetic Acid, $C_2H_4O_2$	3	3	0	0	0	0	3	0	0	0	0	0	0	0	0	0	0	0	0
Butanol, $C_4H_{10}O$	143	143	0	0	0	143	0	0	4	139	0	4	236	41	277	97	179	0	139
Butyric Acid, $C_4H_8O_2$	8	8	0	0	0	1	7	0	0	1	0	0	0	0	0	0	0	1	0
Ethanol, $C_2H_6O_2$	15	15	0	0	0	15	0	0	13	1	0	13	15	7	22	13	8	0	1
H_2O	8,450	8,450	248	248	0	704	7,746	0	9	695	8	8	363	33	395	354	42	686	9
Solids	85	0	0	85	0	0	0	0	0	0	0	0	0	0	0	0	0	0	0
Totals	**8,769**	**8,684**	**248**	**333**	7	**921**	7,756	**5**	**80**	**836**	**61**	**26**	**614**	**81**	**694**	**458**	**229**	**687**	**149**
Temp (°C)	35	35	35	25	35	35	112	35	35	91	35	81	96	91	35	35	35	100	99
Pressure (bar)	2	1	1	1	2	2	2	1	1	1	1	1	1	1	0.07	1	1	1	1

Appendix C: Equipment IDs and Names

C-201	Air Stream Compressor
CB-201	Whey Protein Conveyor Belt
E-101	Acid Whey Preheater
E-102	Permeate Cooling
E-201	Air Stream Heater
E-301	Substrate Heater
E-302	Fermentation Tank Cooler
E-303	Fermentation Tank Cooler
E-304	Fermentation Tank Cooler
E-305	Fermentation Tank Cooler
E-306	Fermentation Tank Cooler
E-307	Fermentation Tank Cooler
E-308	Fermentation Tank Cooler
E-309	Fermentation Tank Cooler
E-310	Fermentation Tank Cooler
E-401	Water Column I Condenser
E-402	Water Column I Reboiler
E-403	Volatiles Column Condenser
E-404	Volatiles Column Reboiler
E-405	Acetone Ethanol Column Condenser
E-406	Acetone Ethanol Column Reboiler
E-407	Water Column II Reboiler
E-408	Butanol Column Reboiler
E-409	Azeotrope Condenser
F-101	Ultrafiltration System
F-201	Air Filter
F-401	Depth Filtration System
H-201	Spray Dryer
P-101 A/B	Acid Whey Pumps
P-102 A/B	Permeate Pumps
P-201 A/B	Wet Whey Pumps

P-301 A/B	Storage Pumps
P-302 A/B	Seed Train Pumps
P-303 A/B	Fermenter Pumps
P-401 A/B	Fermentation Product Pumps
P-402 A/B	Depth Filtration Backwash Pumps
P-403 A/B	Post-Depth Filtration Pumps
P-404 A/B	Water Column I Reflux Pumps
P-405 A/B	Water Column I Bottoms Pumps
P-406 A/B	Volatiles Column Reflux Pumps
P-407 A/B	Volatiles Column Bottoms Pumps
P-408 A/B	Acetone Ethanol Column Reflux Pumps
P-409 A/B	Acetone Ethanol Column Bottoms Pumps
P-410 A/B	Decanter Aqueous Phase Pump
P-411 A/B	Decanter Organic Phase Pump
P-412 A/B	Water Column 2 Bottoms Pumps
P-413 A/B	Butanol Column Bottoms Pumps
R-301	*C. acetobutylicum* Seed Train Unit
R-302	Batch ABE Fermentation Reactor
R-303	Batch ABE Fermentation Reactor
R-304	Batch ABE Fermentation Reactor
R-305	Batch ABE Fermentation Reactor
R-306	Batch ABE Fermentation Reactor
R-307	Batch ABE Fermentation Reactor
R-308	Batch ABE Fermentation Reactor
R-309	Batch ABE Fermentation Reactor
R-310	Batch ABE Fermentation Reactor
R-311	Batch ABE Fermentation Reactor
RO-101 + RO-102	Reverse Osmosis System
T-402	Volatiles Column
T-403	Acetone Ethanol Column
T-404	Water Column II
T-405	Butanol Column

V-101	Acid Whey Storage Vessel
V-201	Whey Protein Product Storage
V-301	Concentrate Permeate Storage
V-401	Fermented Products Flash Unit
V-402	Water Column I Reflux Drum
V-403	Volatiles Column Reflux Drum
V-404	Acetone Ethanol Column Reflux Drum
V-405	Acetone Product Storage
V-406	Butanol Product Storage

Appendix D: Weather Conditions and Chemical Information used in ALOHA Simulation

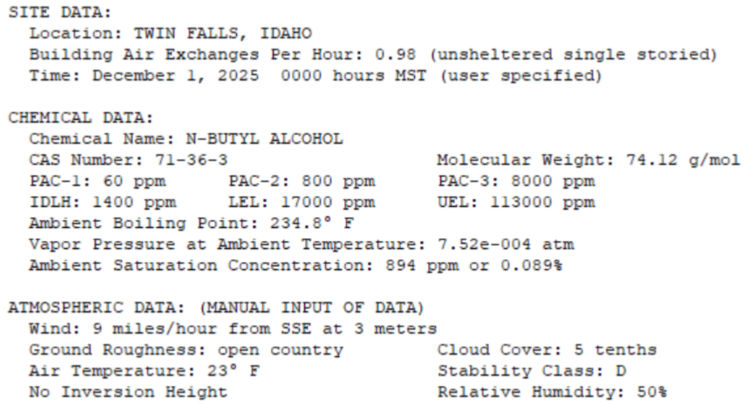

```
SITE DATA:
  Location: TWIN FALLS, IDAHO
  Building Air Exchanges Per Hour: 0.98 (unsheltered single storied)
  Time: December 1, 2025  0000 hours MST (user specified)

CHEMICAL DATA:
  Chemical Name: N-BUTYL ALCOHOL
  CAS Number: 71-36-3                  Molecular Weight: 74.12 g/mol
  PAC-1: 60 ppm      PAC-2: 800 ppm      PAC-3: 8000 ppm
  IDLH: 1400 ppm     LEL: 17000 ppm      UEL: 113000 ppm
  Ambient Boiling Point: 234.8° F
  Vapor Pressure at Ambient Temperature: 7.52e-004 atm
  Ambient Saturation Concentration: 894 ppm or 0.089%

ATMOSPHERIC DATA: (MANUAL INPUT OF DATA)
  Wind: 9 miles/hour from SSE at 3 meters
  Ground Roughness: open country        Cloud Cover: 5 tenths
  Air Temperature: 23° F                Stability Class: D
  No Inversion Height                   Relative Humidity: 50%
```